Atmos. Chem. Phys. Discuss., 15, 23731–23794, 2015
www.atmos-chem-phys-discuss.net/15/23731/2015/
doi:10.5194/acpd-15-23731-2015

Atmospheric Chemistry and Physics Discussions

Assessing the ammonium nitrate formation regime in the Paris megacity and its representation in the CHIMERE model

H. Petetin[1,a], J. Sciare[2,3], M. Bressi[2], A. Rosso[4], O. Sanchez[4], R. Sarda-Estève[2], J.-E. Petit[2,b], and M. Beekmann[1]

[1]LISA/IPSL, Laboratoire Inter-universitaire des Systèmes Atmosphériques, UMR CNRS 7583, Université Paris Est Créteil (UPEC) and Université Paris Diderot (UPD), France
[2]LSCE, Laboratoire des Sciences du Climat et de l'Environnement, CNRS-CEA-UVSQ, Gif-sur-Yvette, France
[3]Energy Environment Water Research Center (EEWRC), The Cyprus Institute, Nicosia, Cyprus
[4]AIRPARIF, Agence de surveillance de la qualité de l'air, Paris, France
[a]now at: Laboratoire d'Aérologie, Université Paul Sabatier and CNRS, Toulouse, France
[b]now at: Air Lorraine, Villers-les-Nancy, France

Received: 6 March 2015 – Accepted: 21 May 2015 – Published: 3 September 2015

Correspondence to: H. Petetin (hervepetetin@gmail.com)

Published by Copernicus Publications on behalf of the European Geosciences Union.

ACPD
15, 23731–23794, 2015

Abstract

Secondary inorganic compounds represent a major fraction of fine aerosol in the Paris megacity. The thermodynamics behind their formation is now relatively well constrained, but due to sparse direct measurements of their precursors (in particular NH_3 and HNO_3), uncertainties remain on their concentrations and variability as well as the formation regime of ammonium nitrate (in terms of limited species, among NH_3 and HNO_3) in urban environments such as Paris. This study presents the first urban background measurements of both inorganic aerosol compounds and their gaseous precursors during several months within the city of Paris. Intense agriculture-related NH_3 episodes are observed in spring/summer while HNO_3 concentrations remain relatively low, even during summer, which leads to a NH_3-rich regime in Paris. The local formation of ammonium nitrate within the city appears low, despite high NO_x emissions. The dataset is also used to evaluate the CHIMERE chemistry-transport model (CTM). Interestingly, the rather good results obtained on ammonium nitrates hide significant errors on gaseous precursors (e.g. mean bias of −75 and +195 % for NH_3 and HNO_3, respectively). It thus leads to a mis-representation of the nitrate formation regime through a highly underestimated Gas Ratio metric (introduced by Ansari and Pandis, 1998) and a much higher sensitivity of nitrate concentrations to ammonia changes. Several uncertainty sources are investigated, pointing out the importance of better assessing both NH_3 emissions and OH concentrations in the future. These results finally remind the caution required in the use of CTMs for emission scenario analysis, highlighting the importance of prior diagnostic and dynamic evaluations.

1 Introduction

Atmospheric particulate matter (PM) consists in a complex mixture of various organic and inorganic compounds known to have serious adverse effects on human health (Chow, 2006; Pope et al., 2009), in particular close to primary sources in urban en-

ACPD
15, 23731–23794, 2015

vironments. Through acidic deposition, it also affects both ecosystems (Camargo and Alonso, 2006; Grantz et al., 2003) and monuments (Lombardo et al., 2013). It plays a crucial but still uncertain role in climate change through interactions with radiation and clouds formation, leading at a global scale to a radiative forcing estimated between -1.9 and $-0.1\,W\,m^{-2}$ at a 95 % confidence interval (IPCC, 2013). Among the various chemical constituents of PM, nitrate (NO_3^-) contributes significantly in the form of semi-volatile ammonium nitrate to the fine (PM with aerodynamic diameter – A.D. – below 2.5 µm) and coarse (A.D. between 2.5 and 10 µm) aerosol modes, with mean contributions in Europe around 6–16 and 6–20 %, respectively (Putaud et al., 2010). Several studies have reported increasing ammonium nitrate contributions with increasing PM mass concentrations in urban sites, thus underlying their importance in exceedances of PM European standards (Putaud et al., 2010; Yin and Harrison, 2008). Such pattern has been evidenced for the city of Paris by Sciare et al. (2010), Bressi et al. (2013) and Petit et al. (2014) and clearly points to the need for a better understanding of the processes controlling the formation of ammonium nitrate.

Ammonium nitrate formation primarily results from both the formation of nitric acid (HNO_3) and the emission of ammonia (NH_3) under favourable thermodynamic conditions. NO_2 is converted in HNO_3 through the oxidation by the OH radical (homogeneous direct pathway) or ozone (through the formation of several intermediate compounds, including nitrate radical NO_3 and nitrogen pentoxide N_2O_5; heterogeneous indirect pathway) (Seinfeld and Pandis, 2006). The first pathway is expected to dominate during daytime, when OH concentrations are the highest (Matsumoto and Tanaka, 1996). Conversely, due to the very short lifetime of the $NO_3^\bullet$ radical in the presence of solar irradiation (Vrekoussis et al., 2004), the second pathway mainly acts during nighttime, favoured by decreasing temperature and increasing relative humidity (RH), or during fog events (Platt et al., 1981; Dall'Osto et al., 2009; Healy et al., 2012). Additionally, some nitric acid may also be directly emitted by both anthropogenic (e.g. industry) and natural (e.g. volcanoes, Mather et al., 2004) sources. Ammonia is mainly emitted by agricultural activities (at 93 % in France, CITEPA, 2013), with several other minor

ACPD
15, 23731–23794, 2015

sources including industry, traffic (e.g. Kean et al., 2009; Bishop et al., 2010; Carslaw and Rhys-Tyler, 2013; Yao et al., 2013) or sewage disposal (Sutton et al., 2000). In the presence of ammonia available after the neutralization of sulfate, a thermodynamic equilibrium is engaged between both gaseous compounds (HNO_3 and NH_3). It potentially leads to the formation of ammonium nitrate in the aqueous or solid phase, depending on temperature, RH and sulfate concentrations (Ansari and Pandis, 1998; Mozurkewich, 1993). In marine environments, nitric acid may also adsorb onto NaCl salts and react to form sodium nitrate ($NaNO_3$) in the coarse fraction (Harrison and Pio, 1983; Ottley and Harrison, 1992). The relationship between nitrate aerosols and its gaseous precursors is thus highly non-linear (Ansari and Pandis, 1998), and the calculation of nitrate concentrations requires the use of thermodynamic models able to determine the partitioning of inorganic compounds between the gaseous and aerosol (aqueous or solid) phases depending on the temperature and RH conditions (see Fountoukis and Nenes, 2007 for a review).

Considering the high contribution of nitrate in fine particulate pollution, both the identification of the limited species (among NH_3 and HNO_3) in the formation of ammonium nitrate and the quantification of the PM response to a given emission reduction of either precursor are crucial information for air quality management authorities in charge of designing efficient PM control strategies. Various approaches have been proposed in the literature to investigate these points, the reliability of results mostly depending on the observational dataset available. As they do not require any measurements, chemistry-transport models (CTMs) simulations and emission reduction scenarios remain the easiest way to provide a first guess of the limited species and PM response to emission changes. Over Europe, several studies with different CTMs have simulated a HNO_3-limited regime (Sartelet et al., 2007; Kim et al., 2011 with the POLYPHEMUS model; Hamaoui-Laguel et al., 2014 with the CHIMERE model; Pay et al., 2012 with the CALIOPE-EU modelling system). However, such an approach relies on the good performance of CTMs that still suffer from various uncertainties, in particular in their input data (e.g. emission inventories). In respect to these per-

ACPD
15, 23731–23794, 2015

spectives, comparisons with field observations are highly valuable for evaluating model outputs. When measurements of total nitrate ($TNO_3 = HNO_{3(g)} + NO_3^-$), total ammonia ($TNH_3 = NH_{3(g)} + NH_4^+$) and total sulfate ($TS = H_2SO_4(g) + SO_3^- + SO_4^{2-}$) are available, it is possible to diagnose which precursor is limited in the nitrate formation. A first approach relies on the use of the gas ratio (GR) defined as the ratio of free ammonia after sulfate neutralization (FNH_x ($\mu mol\,m^{-3}$) $= NH_3 + NH_4^+ - 2xSO_4^{2-}$) over total nitrate ($TNO_3$ ($\mu mol\,m^{-3}$) $= HNO_3 + NO_3^-$) (Ansari and Pandis, 1998). GR values above unity indicate a regime mainly limited by nitric acid (e.g. NH_3-rich regime) in which there is enough NH_3 to neutralize both sulfate and nitrate. Conversely, gas ratios between 0 and 1 indicate that there is enough NH_3 to neutralize the sulfate but not nitrate, while negative ones correspond to a NH_3-poor regime in which NH_3 amounts are insufficient to even neutralize the sulfate. Based on EMEP regional background observations, Pay et al. (2012) have obtained GR above unity (i.e. a HNO_3-limited regime) over continental Europe, in reasonable agreement with the CALIOPE model. Conversely, a NH_3-limited regime was found over ocean and closer to coasts in some countries (e.g. Spain, England, countries around Baltic Sea) due to ship emissions of SO_2 and NO_x and low NH_3 over marine regions. However, the determination of the limited compound based on GR is valid only under the assumption of a complete transfer (of the limited species) in the aerosol phase (i.e. at low temperature and high RH). Under ambient conditions favouring a partitioning between both phases, both ammonia and nitric acid exist in the gas phase and the nitrate formation may be sensitive to changes in one or the other precursor. A more realistic assessment of the nitrate formation regime can be obtained by performing sensitivity tests on thermodynamic models fed by field measurements (concentrations, temperature and RH). Such an approach allows quantifying the PM response to total reservoir (either TNH_3, TNO_3 or TS) concentrations reductions (the link with precursors emissions remaining more difficult to assess without the use of CTMs) (Ansari and Pandis, 1998; Takahama et al., 2004 with the GFEMN model; Blanchard and Hidy, 2003 with the SCAPE2 model). These studies rely on the hypothesis that the concentration reduction of one specific compound does not affect

ACPD
15, 23731–23794, 2015

the others, which is not true due to lifetime differences between gas and aerosol phases induced by contrasted deposition rates; for instance, a reduction of sulfate increases the amount of FNH_x available for the formation of nitrate that deposit less than nitric acid (Davidson and Wu, 1990), which finally increases the TNO_3 reservoir. These difficulties may be overcome through the combined use of observations and deposition parameterizations in observation-based box models (Vayenas et al., 2005). As such models cannot integrate the whole complexity at stake in the atmosphere, CTMs are still needed to assess the nitrate formation regime and the PM response to precursors changes, but require in turn to be validated by experimental data.

This paper aims at investigating the variability and sources of both HNO_3 and NH_3, and the associated ammonium nitrate formation regime in the Paris megacity, as well as the ability of the CHIMERE regional chemistry-transport model to reproduce it. Concerning the investigation of nitrate responses to TNH_3 and TNO_3 decreases, the approach of Vayenas et al. (2005) is probably the most realistic but as it introduces uncertainties through the removal parameterizations, the approach of Takahama et al. (2004) is preferred as a first guess. To answer these questions, an important experimental effort, in the framework of the PARTICULES and FRANCIPOL projects, has recently made available a large database of fine aerosol chemical compounds (e.g. nitrate, ammonium, sulfate) and inorganic gaseous precursors (e.g. nitric acid, ammonia) in the region of Paris. To our knowledge, this is the first time that simultaneous measurements of inorganic compounds in both gaseous and aerosol phases, covering most seasons are performed in France. Experimental aspects are described in Sect. 2. The CHIMERE model and its setup is then introduced in Sect. 3. Results are shown and discussed in Sect. 4, while overall conclusions are given in Sect. 5.

ACPD
15, 23731–23794, 2015

2 Experimental

2.1 Fine aerosols measurements

As part of the AIRPARIF-LSCE "PARTICULES" project (Airparif, 2011, 2012), fine aerosol particles ($PM_{2.5}$) were collected every day during 24 h (from 00:00 to 23:59 LT) during one year (from 11 September 2009 to 10 September 2010) using two collocated Leckel low volume samplers (SEQ47/50) running at 2.3 $m^3 h^{-1}$. One Leckel sampler was equipped with quartz filters (QMA, Whatman, 47 mm diameter) for carbon analyses, the second with Teflon filters (PTFE, Pall, 47 mm diameter, 2.0 µm porosity) for gravimetric and ion measurements (including NH_4^+, NO_3^-, SO_4^{2-}). Six sampling sites were implemented, covering the region of Paris. Only the results for the background station located in the city centre of Paris (4th district, 48°50′56″ N, 02°21′55″ E, 20 m above ground level, a.g.l.) will be presented here. More information on the experimental setup and quality control of the datasets is available in Bressi et al. (2013). Note that filter measurements are subject to artefacts, through the evaporation and/or the adsorption of semi-volatile compounds (Pang et al., 2002), and thus mostly affect ammonium nitrate and organic matter concentrations. Daily chemical mass closure studies and comparisons with on-line artefact-free measurements were performed for that purpose and showed that filter sampling was missing quite systematically about 20 % of $PM_{2.5}$ (15 % of fine nitrate; Bressi et al., 2013).

2.2 Gaseous precursors measurements

As part of the PRIMEQUAL "FRANCIPOL" project, gaseous precursors (NH_3, HNO_3, SO_2) were monitored in near real-time on the roof platform at the Laboratoire d'Hygiène de la Ville de Paris (LHVP) in the heart of Paris (13th district), which is regarded as being representative of the background pollution of the city of Paris (Favez et al., 2007).

Gas-phase ammonia measurements were obtained for a 10 month period (May 2010–February 2011) every 5 min using an AiRRmonia monitor (Mechatronics

ACPD
15, 23731–23794, 2015

Instruments BV, the Netherlands). The March/April periods (2010 and 2011) were missing due to technical problems of the instrument. Based on conductivity detection of NH_4^+, gaseous NH_3 is sampled at 1 L min^{-1} using a 1 m long Teflon (1/2 inch diameter) sampling line. Then, it is collected through a sampling block equipped with an ammonia-permeable membrane; a demineralized water counter-flow allows NH_3 to solubilize in NH_4^+. A second purification step is applied by adding 0.5 mM sodium hydroxide, leading to the detection of NH_4^+ in the detector block. The instrument has been calibrated regularly (twice per months) using 0 ppb and 500 ppb NH_4^+ aqueous solution (NIST standards). Two sets of sampling syringes ensure a constant flow throughout the instrument, but also create a temporal shift, ranging from 10 to 40 min by different studies (Erisman et al., 2001; Cowen et al., 2004; Zechmeister-Boltenstern, 2010; von Brobrutzki et al., 2010). We have taken here a constant value of 30 min for this delay in time response. Detection limit and precision of the instrument are typically 0.1 µg m^{-3} and 3 to 10 %, respectively (Erisman et al., 2001; Norman et al., 2009). More than 62 000 valid data points of NH_3 – covering 217 days – were obtained with the AiRRmonia instrument and used for this study.

Nitric acid and sulfur dioxide were analyzed continuously for an 11 month period (March 2010–January 2011) using a Wet Annular Denuder (WAD) similar to the one reported in details by Trebs et al. (2004) and coupled with Ion Chromatography (IC). Briefly, whole air is sampled at ∼ 10 L min^{-1} in the WAD. This air flowrate – slightly below the 17 L min^{-1} usually set – was taken to ensure a laminar flow and minimize particle losses onto the walls of the WAD and thus minimize possible artefacts in our IC (anion) measurements that could raise from inorganic salts present in the particulate phase. Following the recommendations by Neuman et al. (1999), our sampling line were made of plastic (PE, 1/2 inch diameter, John Guest, USA) and reduced to 1 m in order to keep a residence time of sampled air below 1 s preventing formation/losses of ammonium nitrate (Dlugi, 1993). 18.2 MΩ water was used to rinse the WAD at a flowrate of ∼ 0.40 mL min^{-1} and feed the IC with the solubilized acid gases. The IC (ICS2000, Dionex) configuration setup is similar to the one reported by (Sciare et al.,

ACPD
15, 23731–23794, 2015

2011). Time resolution (chromatogram) was typically 15 min for the major gaseous acidic species (HCOOH, CH_3COOH, HCl, HONO, HNO_3, SO_2). Oxidation of SO_2 into SO_4^{2-} in the liquid flow downstream of the WAD was performed by solubilization of ambient oxidants such as H_2O_2. Based on these settings, detection limit for acidic gases was typically below 0.1 $\mu g\,m^{-3}$. Uncertainties in ambient concentrations of acidic gases depend on air and liquid flowrates (controlled on a weekly basis) as well as the IC calibration (performed every 2 months). Overall standard deviations (1σ) of 6, 15 and 10 % were calculated for these 3 parameters (air flowrate, liquid flowrate, IC calibration), respectively, leading a total uncertainty of about 20 % for the WAD-IC measurements.

This WAD technique been successfully intercompared with off-line techniques in (Trebs et al., 2008). Further comparison of the WAD-IC technique was performed during our study with a commercially available SO_2 analyzer (AFM22, Environnement S.A.) for a period of 3 months. Despite the poor detection limit (1 ppb = 2.43 $\mu g\,m^{-3}$) of the commercially available instrument and the low ambient concentrations recorded at our station with SO_2 monthly means ranging from 0.76 to 3.03 $\mu g\,m^{-3}$ measured with our WAD-IC instrument, quite consistent results were obtained from this intercomparison (slope of 0.73 and $r^2 = 0.56$ for $n = 1671$ hourly averaged data points). More than 24 000 valid data points of SO_2 and HNO_3 – covering 253 days – were obtained with the WAD-IC instrument and used for this study.

2.3 Meteorological parameters measurement

Beside chemical compounds, traditional meteorological parameters – temperature, wind speed and direction, RH – are also measured at the MONTSOURIS station (2.337° E, 48.822° N) in Paris, close to the LHVP site (~ 2 km). In addition, boundary layer height (BLH) estimations are retrieved from an aerosol lidar at the SIRTA (*Site Instrumental de Recherche par Télédetection Atmosphérique*) site (48.712° N, 2.208° E) (Haeffelin et al., 2011).

ACPD
15, 23731–23794, 2015

This paper will focus on measurements performed from the 1 April to 31 December 2010. Note that all the measurements described in previous sections come from different campaigns and measurement periods that do not entirely overlap, as shown in Table 1.

3 Model setup and input data

3.1 CHIMERE model description

Simulations are performed with the CHIMERE chemistry-transport model (Schmidt and Derognat, 2001; Bessagnet et al., 2009; Menut et al., 2013) (www.lmd.polytechnique.fr/chimere) designed to provide short-term predictions of ozone and aerosols, as well as to help emissions mitigation assessment through emission reduction scenarios. It is used both in research activities and operational air quality survey and forecasting at the local, national and European scale (ESMERALDA over the northern part of France; PREVAIR service, www.prevair.org; GMES-MACC program).

The CHIMERE model includes the MELCHIOR2 chemical mechanism (around 40 species and 120 reactions) for the gas-phase chemistry, some aqueous-phase (e.g. aqueous pathways for sulfate production) and heterogeneous (e.g. nitric acid formation on existing particles and fog droplets) reactions, and size dependent aerosol compounds (9 bins ranging from 40 nm to 20 µm diameters), including secondary organic and inorganic aerosols. Dry and wet deposition of gaseous and aerosol species is parameterized following the resistance analogy (Wesely, 1989). The model also includes a parameterization of coagulation, absorption and nucleation aerosol processes.

Inorganic species are treated using the ISORROPIA thermodynamic equilibrium model (Nenes et al., 1998), considering only the NH_3-HNO_3-H_2SO_4-H_2O system. The ISORROPIA follows a bulk aerosol approach (without any consideration of the aerosol size distribution) and assumes an instantaneous equilibrium in the gas-aerosol system, as well as no influence of other compounds (in particular, the soluble organic

ACPD
15, 23731–23794, 2015

matter). Given the temperature, relative humidity, total nitrate TNO_3, total ammonia TNH_3 and sulfate (assuming that $TS = SO_4^{2-}$ due to low concentrations of H_2SO_4 and HSO_3 in the aerosol phase), the partitioning coefficient between both aerosol and gas phases at equilibrium is computed and used to drive the system toward the corresponding direction (thus countering the hypothesis of an instantaneous equilibrium assumed in ISORROPIA). For calculation efficiency, the model is not used on-line but through a tabulated version designed to cover a large range of meteorological conditions with temperature ranging from 260 to 312 K (increment +2.5 K), RH from 0.3 to 0.99 (increment +0.05) and sulfate, total nitrate and total ammonia concentrations from 10^{-2} to 65 $\mu g\,m^{-3}$ (increment ×1.5) (Menut et al., 2013).

3.2 Model configuration

As shown in Fig. 1, three nested domains are considered in all simulations – a large (LAR), a medium (MED) and a fine (FIN) domain –, with horizontal resolutions increasing from 0.5° × 0.5° (roughly 50 km × 50 km), 9 km × 9 km and 3 km × 3 km, respectively. A discretization of eight levels, from 40 m to 5 km a.g.l., is applied on the vertical dimension.

Meteorological inputs are taken from PSU/NCAR MM5 simulations (Dudhia, 1993) using boundary conditions and large scale data coming from Final Analyses (FNL) data from National Centers for Environmental Prediction (NCEP).

Gaseous and aerosol emissions in all domains come from the so-called TNO-MP (MP for MegaPoli) inventory. Developed in the framework of the European MEGAPOLI (Megacity: emission, urban, regional and global atmospheric pollution and climate effect, and integrated tools for assessment and mitigation; www.megapoli.info) project (Baklanov et al., 2010), this highly-resolved (0.125° × 0.0625°, i.e. roughly 7 km × 7 km) European inventory is based on the TNO inventory (Gon et al., 2010; Pouliot et al., 2012; Kuenen et al., 2014), but incorporates bottom-up emission data (compiled by local authorities such as Airparif for Paris, Airparif, 2010) over the four European megacities (Paris, London, Rhine-Ruhr and Po valley) (see Denier van der Gon et al., 2011, for

ACPD
15, 23731–23794, 2015

more details). The region of Paris roughly corresponds to the FIN domain. In order to reach the CHIMERE resolution, emissions are downscaled based on the 1 km × 1 km-resolved GLCF (Global Land Cover Facility) land use database (Hansen et al., 2000), and apportioned according to the type of land use (Menut et al., 2013).

Boundary and initial conditions come from the LMDz-INCA2 (Folberth et al., 2006) global model for gaseous species and the LMDZ-AERO (Folberth et al., 2006; Hauglustaine, 2004) for particulate species. Biogenic emissions are computed from the MEGAN model using parameterizations from Guenther et al. (2006).

This reference simulation will be referred to as the MOD case. A second simulation is performed without any local anthropogenic emissions from the region of Paris (in the three nested domains), in order to assess the influence of imported pollution over the city of Paris. It will be referred to as the MOD-noIDF case (IDF for Ile-De-France which design the name of the region of Paris). In addition, a third simulation (so-called MOD-nodep) is performed without any NH_3 dry deposition over the entire domain.

4 Results

The following sections present results on sulfate and SO_2 (Sect. 4.1), ammonia (Sect. 4.2) and nitric acid (Sect. 4.3). For all compounds, the temporal variability given by measurements is assessed at different scales (monthly, daily and diurnal), as well as the model ability to reproduce field concentrations. For the analysis of air mass origins, back-trajectories have been calculated during the whole period with the FLEXTRA model (Stohl et al., 2001) using the same MM5 meteorology already used in the CHIMERE simulations, calculations being performed every 6 h with 10 particles distributed around the centre of Paris, which leads to a daily set of 40 back-trajectories. Several uncertainty sources in the model (or input data) are also discussed. The nitrate formation regime in terms of limiting species among NH_3 and HNO_3, the nitrate simulation in CHIMERE as well as the nitrate response to changes in precursors concentrations are then characterized in Sect. 4.4.

ACPD
15, 23731–23794, 2015

Statistical metrics used in the evaluation of the CHIMERE results compared to field observations are defined as follows:

$$\text{Mean bias: MB} = \frac{1}{n}\sum_{i=1}^{n}(m_i - o_i) \quad (1)$$

$$\text{Normalized mean bias: NMB} = \frac{\frac{1}{n}\sum_{i=1}^{n}(m_i - o_i)}{\overline{o}} \quad (2)$$

$$\text{Root mean square error: RMSE} = \sqrt{\frac{1}{n}\sum_{i=1}^{n}(m_i - o_i)^2} \quad (3)$$

$$\text{Normalized root mean square error: NRMSE} = \frac{\sqrt{\frac{1}{n}\sum_{i=1}^{n}(m_i - o_i)^2}}{\overline{o}} \quad (4)$$

$$\text{Correlation coefficient: } R = \frac{\sum_{i=1}^{n}(m_i - \overline{m})(o_i - \overline{o})}{\sqrt{\sum_{i=1}^{n}(m_i - \overline{m})^2 \sum_{i=1}^{n}(o_i - \overline{o})^2}} \quad (5)$$

With m_i and o_i being the modelled and observed concentrations at time i, respectively, and $\overline{m}$ and $\overline{o}$ their average over a given period.

4.1 Sulfate and SO_2

Sulfate daily concentrations in Paris are given in Fig. 2. The variability of sulfate (as of nitrate) during the PARTICULES campaign has been discussed in details in Bressi et al. (2013). Fine ($PM_{2.5}$) sulfate concentrations range between 0.4 and 5.0 $\mu g\,m^{-3}$ (plus one high value at 8.7 $\mu g\,m^{-3}$), with an average of 2.0 $\mu g\,m^{-3}$ over the studied period (1 April–10 September, see Table 1). The episodes with highest concentrations are associated to air masses originating from the North/North-East, as previsouly noticed by Bressi et al. (2013), Petetin et al. (2014) and Petit et al. (2014). Despite a faster

ACPD
15, 23731–23794, 2015

SO_2-to-sulfate conversion due to higher OH levels in summer, lower concentrations are measured during that season due to a combination of lower SO_2 emissions and a dominant marine regime, with relatively clean air masses originating from West and South-West and slightly more polluted ones from North-West.

During the period of available data (152 days in spring and summer), ammonia levels are high enough to fully neutralize both sulfate and nitrate, as indicated by the linear regression of NH_4^+ vs. $NO_3^- + 2SO_4^{2-}$ daily concentrations in the fine mode that gives a slope of 1.01, a y intercept of −0.20 ppb and a correlation coefficient (r^2) of 0.97 (n = 150; see Fig. S1 in the Supplement). Note that plotting all major cations ($Na^+ + NH_4^+ + K^+ + 2Ca^{2+} + 2Mg^{2+}$) against all major anions ($NO_3^- + 2SO_4^{2-} + Cl^-$) leads to a slope of 1.03, a y intercept of +0.13 ppb and a correlation of 0.97, demonstrating the neutrality of our fine aerosols.

Statistical results of modelled vs. measured concentrations are reported in Table 2. The model reasonably reproduces the day-to-day variability of sulfate concentrations (r = 0.59), but gives overestimated concentrations, with a mean bias of +48 % and a NRMSE of 74 %. This does not appear to be related to a too high SO_2-to-sulfate conversion since SO_2 concentrations are significantly overestimated in Paris, by about a factor of 3 (Table 2). Additionally, as illustrated in Fig. 3, the S ratio – defined as the ratio of SO_2 over SO_2 plus sulfate, all concentrations being expressed in µg m^{-3} (Hass et al., 2003; Pay et al., 2012) – is also overestimated by the model (0.54 against 0.34, i.e. a positive bias of +60 %). CHIMERE simulates too much freshly emitted SO_2, compared to reality.

Such a high bias on SO_2 concentrations is not expected, but does not appear representative of the CHIMERE performance at a larger scale. Compared to SO_2 observations available at nine urban background sites (AIRPARIF operational network) in the region of Paris, biases calculated from CHIMERE simulations are lower, ranging from +24 to +160 %. As a large part of SO_2 is emitted by point sources, the dilution effect in a 3 km × 3 km cell remains a well-known uncertainty source at stations potentially impacted by plumes coming from nearby industrial facilities. However, in our case,

ACPD
15, 23731–23794, 2015

large SO_2 industrial point sources are relatively far from our background urban station, and emissions from non-point sources (i.e. emissions in road transport and residential sectors) remain important in the center of Paris, which suggests potential errors on the Paris agglomeration emissions (overestimation of total emissions, wrong vertical allocation) and/or the boundary layer height. Indeed, the average SO_2 diurnal profile shows maximum discrepancies (up to a factor of 4.8) during the transition from a convective to a nocturnal boundary layer. As this transition occurs too early in the model (see Fig. S3 in the Supplement), this likely explains a noticeable part of the bias on SO_2. Conversely, the sulfate overestimation may be due to errors during the transport of air masses from North-Eastern Europe.

4.2 Ammonia

4.2.1 Temporal variability

Ammonia daily concentrations and diurnal profiles are given in Fig. 2. The model results will be discussed in the next section. The average concentration of 4.0 ppb measured over the whole period is in the middle range of NH_3 concentrations reported by Reche et al. (2012) in worldwide urban environments ranging between 0.4 and 63.6 ppb (i.e. spanning over two orders of magnitude). It is also consistent with the values obtained in other European cities: 4.4 ppb in Aveiro (Portugal, August–May), 5.2 ppb in Roma (Italy, May–March), 5.5 ppb in Münster (Germany, May–June), 3.2 in Thessaloniki (Greece, year), 3.9–10.6 in Barcelona (Spain, July and January), 3.1 ppb in Schiedam (the Netherlands, winter) (Reche et al., 2012 and references therein). Our NH_3 concentrations in Paris show a large variability (illustrated by a standard deviation of 2.8 ppb) with several intense episodes in late spring and early summer (hourly concentrations reaching up to 18.5 ppb in June), and a decrease in autumn and winter. Such a seasonal pattern has been already reported in many studies (e.g. Reche et al., 2012; Skjøth et al., 2011) and appears mainly due to the intensity of agricultural emissions (maximum during spring) and the influence of temperature (e.g. Perrino et al.,

ACPD
15, 23731–23794, 2015

2002; Plessow et al., 2005) and RH conditions (Nimmermark and Gustafsson, 2005). As shown in Fig. 4, this influence of temperature on NH_3 levels appears clearly in Paris, with highest episodes concomitant of warmest conditions (see the meteorology evaluation in the Supplement, Sect. S2). The lower sensitivity to temperature in the model will be discussed later.

This can be illustrated by the early July episode when, in parallel with the temperature increase between 30 June and 2 July, the NH_3 baseline progressively increases in Paris, up to 18.5 ppb at the hourly scale (the maximum over the whole FRANCIPOL period). Ammonia appears also to be driven by transport patterns and the degree of dispersive conditions. During the first days, clean oceanic air masses are advected towards Paris, but pass over several agricultural regions (e.g. Picardie in Northwest of Paris, Champagne-Ardenne in the East, Burgundy in the Southeast and Centre in the Southwest). This allows enrichment in NH_3 of air masses during their transport over land (given that backtrajectories generally stay within the height of the atmospheric boundary layer). Surprisingly, despite the arrival of a cold front on the 2 July (with lower temperatures and higher RH), NH_3 concentrations keep increasing during the night. During the following days, higher wind speeds (at least in altitude), from the Southwest (3 July morning) and then from the West (3 July, afternoon and 4 July), lead to a decrease of NH_3 concentrations in Paris, despite still high temperatures on the 4 July. A part of the NH_3 increase may be due to evaporation of ammonium nitrate, but in early July, a similar episode is observed on TNH_3. This specific episode thus suggests the presence of intense NH_3 emissions in the East and Southeast of the region of Paris. Back-trajectories during the 10 days of highest NH_3 concentrations (daily averages above 9.2 ppb, the 95th percentile of all daily values) are presented in Fig. 5a. Most of NH_3 episodes are associated to moderate winds in altitude, air masses at D-1 (one day before reaching Paris) being located in a radius of 50–400 km from Paris. A noticeable exception is found on 9 July in the morning (around 06:00 UTC) when the wind suddenly changes direction (from Southeast to Southwest) and speed (getting much stronger, with air masses originating from Spain at D-1) while NH_3 concentrations

ACPD
15, 23731–23794, 2015

increase. Therefore, ammonia episodes in Paris appear closely linked to anticyclonic circulations with associated high temperatures and moderate wind speeds, and not to a specific emitting source region. This is in accordance with the results obtained by Petit et al. (2014) at the SIRTA suburban site (south-west of Paris) that suggest a diffuse regional NH_3 source, in particular during summer (in spring, some high NH_3 episodes associated to E/NE/SE winds are also noticed, but without any clear pattern).

Assuming that concentrations of secondary inorganic compounds (nitrate, sulfate, ammonium) are similar at both LHVP and PAR urban background sites – i.e. (i) any of the two sites are impacted by very local emissions and (ii) the background is homogeneous over that part of Paris –, one can compute daily total ammonium TNH_3 and total nitrate TNO_3. The first hypothesis is supported by the fact that both sites are located on the roof of rather high buildings (around 20 m a.g.l.). The second hypothesis of homogeneous concentrations over Paris is supported by the fact that during the period, inorganic particulate compounds in Paris (nitrate, sulfate, ammonium) are mostly advected from outside the Paris region (Bressi et al., 2013; Petetin et al., 2014). Additionally, both sites are separated by only 3 km, which limits discrepancies in meteorological conditions. As shown in Fig. 6, the experimentally determined TNH_3 is clearly dominated by ammonia that has a contribution around 55–99 % (83 % on average) (again, model results are discussed in the next section). Negative artefacts on ammonium filter measurements cannot be excluded (in particular during summertime), but increasing ammonium concentrations by 50 % has a very limited impact (NH_3 contributions ranging in that case around 45–99, and 78 % on average). Thus, ammonia episodes cannot be explained by evaporation of ammonium and are likely due to higher land emissions. As agricultural activities are expected to be the main emission source, the variability of NH_3 concentrations is mostly determined by the variability of fertilizer application, followed by the variability induced by environmental factors (in particular, temperature), and finally by transport. Besides the increase of agricultural ammonia emissions (by volatilization), high temperatures in spring and summer are usually associated with anticyclonic conditions with low wind speeds, favouring NH_3 accumulation. Despite still

ACPD
15, 23731–23794, 2015

high temperatures, the lower concentrations in the second half of July and in August are likely due to reduced use of mineral fertilizers from agriculture activities.

On average, the observed NH_3 diurnal profile (Fig. 2) is rather flat, with slightly increasing concentrations in the morning leading to a maximum at 09:00–10:00 UTC, and lower concentrations in the afternoon. The diurnal variability of ammonia depends on many factors, including the strength of local (agriculture) emission sources, the dry deposition, the evolution of the boundary layer height, the formation of ammonium nitrate during the night promoted by larger relative humidity and thermodynamically driven evaporation of this ammonium nitrate during the daytime (Wichink Kruit et al., 2007). The maximum NH_3 value in the morning has already been reported in other studies, both in an agricultural area (Ontario, Canada by Ellis et al., 2011) and in urban environments (in Singapore, Behera et al., 2013). As ammonia concentrations far from sources are expected to be higher in the residual boundary layer than in the stable nocturnal one (where dry deposition is not compensated by local emissions), the observed increase of NH_3 in the morning may be caused by an entrainment of ammonia into the developing mixing layer (Saylor et al., 2010). Here, the diurnal profile does not show a clear peak at morning rush hours, even during periods of lower agricultural emissions (e.g. August and September; too few data in winter), which suggests that traffic emissions are probably a minor source compared to agriculture during our study. This is supported by the low correlation of BC and NH_3 concentrations measured at the LHVP site (r = 0.20 over the whole period). However, during the end of June episode, the hourly time series shows some morning peaks (above an increasing background line likely due to the advection of agricultural ammonia) that may be associated to traffic NH_3 emissions, as illustrated by the increased correlation with BC (r = 0.60 between the 21 June and 3 July) (Fig. 7). In Roma, Perrino et al. (2002) have observed high levels of NH_3 at kerbside sites with a diurnal profile clearly influenced by traffic emissions. However, due to the combined action of dry deposition, dilution after emissions as well as the conversion into particulate ammonium (with sulfates and/or nitrates), these concentrations were severely reduced at the urban background scale, about a factor

ACPD
15, 23731–23794, 2015

of 5, and the traffic profile type had disappeared. As a result, our urban background conditions may have prevented us to assess accurately the potential impact of traffic emissions on ambient ammonia concentrations. Investigating the NH_3 diurnal variability at the SIRTA site, Petit et al. (2014) noticed a bimodal trafic-like variation but only during spring and not during summer and winter when trafic emissions yet also exist, suggesting that these variations may be related to other processes than trafic.

4.2.2 Model results

As shown in Fig. 2, ammonia concentrations are significantly underestimated by the CHIMERE model with a mean bias (MB) of −75 % (see statistical results in Table 2). This negative bias not only affects the intense peaks but also the baseline concentrations. In their evaluation of the CALIOPE-EU modelling system, Pay et al. (2012) have reviewed the statistical results of various regional models over Europe (during a whole year for most models). As our study does not cover a whole year, statistical results are not directly comparable, but somes figures are still given to shed light on the performance of out CHIMERE simulation. The negative bias in our study is in the range of those reported from the aforementioned study where negative biases spread from −15 to 82 %. Our RMSE (3.9 ppb) is among the best values reported by Pay et al. (2012) (1.6 ppb for the CALIOPE-EU model and 7.6–10.6 ppb for the six other models), as well as the correlation (0.42 against 0.05–0.56). Nevertheless, the CHIMERE model dramatically fails to reproduce the strong spring and summer episodes (and consequently the seasonal variation) during which negative biases on daily concentrations can exceed a factor of 10, despite a monthly distribution giving maximum emissions between March and May (spring fertilizer application).

The quite similar results obtained in the MOD and MOD-noIDF cases indicate that most of the simulated ammonia originates from outside the region of Paris. Concentration maps show that simulated NH_3 concentrations closely follow the spatial distribution of emissions, with maximum levels over Brittany, North of France and Benelux. Due to both dilution and deposition, ammonia concentrations quickly decrease with distance

ACPD
15, 23731–23794, 2015

from these source regions. However, the simulated ammonia lifetime appears high enough to allow imports over the region of Paris. As an illustration, highest simulated concentrations in the city (4.5 ppb, the 29 April) result from an advection of air masses from Eastern Brittany and South-West during the month of maximum emissions (according to monthly factors applied to emissions).

As shown in Fig. 6, the fraction of NH_3 in total ammonia (TNH_3) simulated by CHIMERE is highly variable, ranging from less than 5 to about 90 %, in contradiction with observations which show a clear gas phase reservoir during spring and summer (at around 60–100 %). Our overestimated modelled sulfate concentrations (see Sect. 4.1) may directly reduce the amount of ammonia available in the gas phase. However, the bias on TNH_3 is only reduced to −56 % (against −76 % for NH_3 alone), which indicates that only a minor part of the negative bias on ammonia can be explained by an erroneous partitioning between both gas and aerosol phases (including errors related to sulfate). The meteorological analysis at the MONTSOURIS station shows (between observations and the model) a negative bias on temperature (−1.6 °C) and a positive one on relative humidity (+5.9 % in absolute) (see Sect. S2 in the Supplement), which favours the formation of NH_4^+ and thus decreases gaseous NH_3 in TNH_3. However, correcting these errors in the ISORROPIA model (i.e. replacing the simulated temperature and RH values by the field measurements, without modifying TNH_3, TNO_3 and TS concentrations) does not fill the gap with observations, the average NH_3 concentrations being increased by only 7 % on average.

As previously mentioned, road transport also emits NH_3 and may contribute to our urban background levels in Paris. These road transport emissions are missing in the TNO-MP inventory (see Table S3 in the Supplement), which may induce an underestimation of modelled NH_3 concentrations. The contribution of traffic to ambient NH_3 levels in urban environments is highly variable from one city to another, as illustrated by the $NH_3/(NH_3 + NO_x)$ emission molar ratios that range from a few percent (Yao et al., 2013) to a few tens of percent (Bishop et al., 2010) which are due to differences in the vehicle fleet (Carslaw and Rhys-Tyler, 2013). Sensitivity tests were performed with

ACPD
15, 23731–23794, 2015

added NH_3 traffic emissions and showed reduced bias but did not improve correlation between modelled and measurements, which prevents us from concluding on the importance of these traffic emissions on NH_3 urban background levels.

A large part of the model errors probably arises from the representation of NH_3 air–surface exchanges (emissions and deposition) in the CHIMERE model. This representation is simplified in several respects: the parameterization of NH_3 dry deposition is uni-directional, not taking into account the compensation with emissions; emissions are temporally disaggregated based on monthly, day-of-the-week and diurnal factors without taking into account any environmental factor (e.g. air temperature, soil moisture, agricultural practices). Thus, the model fails at reproducing the significant correlation between NH_3 concentration and daily temperature ($r = 0.52$ against 0.72 in observations), as illustrated in Fig. 4. In light of our comparison, NH_3 emissions parameterization in CHIMERE cannot represent the high spatio-temporal variability of NH_3 emissions, and in particular fails in reproducing the large NH_3 peak values observed in the field. Indeed, these emissions result from very complex mechanisms in which numerous environmental parameters are involved, including the amount of nitrogen fertilizers used over the land; temperature, moisture and pH of the soil; the amount of soluble carbon; the soil disturbance and compaction; fertilization methods (Ma et al., 2010; and references therein). More elaborated parameterizations of NH_3 bi-directional fluxes have been proposed to better handle emission and deposition processes in chemistry-transport models (Massad et al., 2010; Zhang et al., 2010; Pleim et al., 2013). Hamaoui-Laguel et al. (2014) have simulated more realistic NH_3 emissions over France during the spring 2007 by combining the one-dimensional mechanistic model VOLT'AIR (Garcia et al., 2011; Génermont and Cellier, 1997) with agricultural practice and soil data. They have shown a spatial variability of NH_3 emissions mainly driven by the soil pH and the types and rates of fertilization, while the temporal variability was rather driven by meteorological conditions and fertilization dates. Compared to the EMEP inventory (quite similar to TNO-MP for NH_3 emissions), the emissions computed with the VOLT'AIR mechanism appear lower over the Brittany (in the West

ACPD
15, 23731–23794, 2015

of France) and higher over the North of France (around a factor of 2–3). This would suggest a possible underestimation of agricultural NH_3 emissions close to the region of Paris.

Dry deposition of NH_3 and wet deposition of NH_4^+ (after NH_3-to-NH_4^+ conversion) represent the two major sinks for ammonia and ammonium, respectively; the first being dominant near emission sources whereas the second dominates at a larger scale (Asman et al., 1998). Uncertainties in the parameterization of both dry and wet deposition in the CHIMERE model may thus explain partly the modelled ammonia underestimation. Results from the MOD-nodep sensitivity test (with no ammonia dry deposition) allow assessing an upper bound of uncertainties related to dry deposition. On average, more than half of the ammonia reaching Paris is deposited in the MOD case, as illustrated by the increase of NH_3 concentrations by a factor of 2.2 when deposition is removed. The diurnal profile indicates that deposition in CHIMERE mostly affects night-time concentrations, likely due to the shallow boundary layer. Despite the unrealistic character of this sensitivity test (dry deposition being one of the dominant NH_3 sinks), this appears not sufficient to increase concentrations towards observed ambient levels (NMB of −46 %). Then, deposition does not appear as the major uncertainty source in the CHIMERE simulated NH_3.

4.2.3 Conclusions on ammonia

Our ammonia urban background measurements in the Paris megacity have highlighted several intense episodes during spring and early summer during anticylonic conditions with high temperature, increasing agricultural emissions and moderate winds enabling an accumulation of ammonia and a subsequent advection over the city. Significant negative biases on ammonia have been found in the CHIMERE model, for the baseline concentrations and for the intense episodes as well as for the hourly variability. Errors in the partitioning of TNH_3 between gas and aerosol phases (due to errors in modelled sulfate, nitrate or local meteorology) as well as uncertainties on deposition can only explain a minor part of the bias. Thus, simulated ammonia concentrations appear

ACPD
15, 23731–23794, 2015

mainly affected by uncertainties in emissions, and in particular the lack of dynamical treatment of agricultural emissions as a function of environmental factors (temperature, etc.). Note that these errors may be even larger in March when NH_3 emissions are the highest but due to instrumental problems, measurements during that period were too sparse to allow a relevant comparison with CHIMERE.

4.3 Nitric acid

4.3.1 Temporal variation

Nitric acid concentrations and their diurnal profile are shown in Fig. 2. Over the whole period, the average HNO_3 concentration is 0.25 ppb. Several moderate episodes are observed in spring and early summer, with daily concentrations up to 1.2 ppbv at the beginning of July. This leads to a seasonal pattern characterized by higher values in spring/summer compared to autumn/winter. Such temporal variations are expected in urban environments close to NO_x emissions due to both the higher OH production in summer and the higher temperatures (as well as the lower RH) that prevent the condensation of HNO_3 (into particulate nitrate), and are consistent with other studies in urban locations (Cadle et al., 1982; Cadle, 1985 in Warren, Michigan, United States, US; Solomon et al., 1992 in Los Angeles, California, US; Perrino et al., 2002 in Roma, Italy).

In Paris the highest HNO_3 episodes are associated with high temperatures and low-to-moderate wind speeds at ground. These conditions increase the atmospheric stratification and the residence time of NO_x emissions over the agglomeration and allow for a more efficient HNO_3 formation via the $NO_2 + OH$ reaction (as confirmed by many black carbon episodes preceding HNO_3 peaks). This is illustrated during the first days of June in Fig. 8. The 1 June is characterized by low wind speed but cloudy conditions that decrease the photooxidation rate of NO_x. Temperature progressively increases during the next two days, but high wind speeds prevent accumulation of HNO_3. Both conditions – moderate wind speed and high temperature, up to 30 °C on hourly aver-

ACPD
15, 23731–23794, 2015

age – are sufficient the 4 and 5 June to lead to significant photochemical driven diurnal variation of HNO_3 with peaks above 1.5 ppb in the afternoon. Some HNO_3 is also probably (slowly) advected by north-east winds but the strong diurnal variability suggests that this contribution is minor in comparison to local formation. The episode ends with a significant decrease of temperature in parallel to more dispersive conditions.

Such episode with strong diurnal variations and amplitudes connected to local meteorological conditions thus suggests a dominant local contribution for HNO_3. Model results will be commented in the next section but it is worthwhile noting at this stage that this specific result is consistent with the CHIMERE simulations that give for the 5 June one of the highest relative contribution of local HNO_3 production, around 70 %; this contribution being determined by the MOD-noIDF to MOD ratio related to total TNO_3 (considering that TNO_3 formation, contrary to HNO_3, is not affected by changes in the thermodynamic equilibrium due to the absence of emissions in MOD-noIDF). Note that, despite the high uncertainties at stake in the simulation of HNO_3 and TNO_3 (as it will be discussed in Sect. 4.3.2), meteorological input data appear reliable and the model thus remains useful to identify such very low dispersive conditions. Although local weather conditions prevail on HNO_3 formation, the contribution of imports – as modelled by CHIMERE – for the 4 to 5 June remains still noticeable and is associated to the (slow) advection of continental air masses originating from Benelux and western Germany which are strong NO_x emitters. More generally, north/north-east winds in Paris are associated with higher HNO_3 concentrations, as shown by the pollution rose (see Fig. S4 in the Supplement), which suggests a substancial contribution of imports. This pattern can be seen the 3 June (and to a lesser extent the day before) when HNO_3 Paris concentrations are mainly driven by imports from the north (90 % in the model). However, according to the back-trajectories related to the highest HNO_3 daily concentrations (Fig. 5b), these episodes appear to be related to very different air mass origins, without any clear dominant sector (while a north-east dominant sector would have been expected, considering the high NO_x emissions in Benelux region and the shape of the pollution rose). These elements thus suggest that imports may be

ACPD
15, 23731–23794, 2015

an important source of HNO_3 in Paris, except during some specific episodes where meteorological conditions allow a mainly local formation.

In terms of diurnal variability (Fig. 2), the ratio between daytime and nighttime HNO_3 concentrations is close to a factor of 2 on average (despite the development of the convective boundary layer in the afternoon). As for ammonia, the concentration of HNO_3 decreases in the early morning, which may be explained by dew formation processes that allows the absorption of water-soluble gases such as HNO_3 (Mulawa et al., 1986; Parmar et al., 2001; Pierson et al., 1988).

Nitric acid accounts for 51 % of total nitrate on average (Fig. 9) but this ratio appears highly variable. The lowest HNO_3/TNO_3 ratios (a few %) are observed during cold days in mid-May when daily temperatures fall below 8 °C (see Fig. S2 in the Supplement), while the highest ratios occur during early summer, with values up to 96 %. As discussed later, the impact of temperature on thermodynamic equilibrium is seen here. Despite high temperatures, low ratios (below 40 %) are also observed on specific periods during summer, particularly in August, when TNO_3 concentrations are low. Such pattern may be due to high measurement uncertainties occurring for low TNO_3 concentrations.

4.3.2 Model results

Nitric acid concentrations are significantly overestimated by CHIMERE, with a NMB of +195 %, leading to a large error (NRMSE of 320 %), in particular at mid-day where the bias can reach a factor of 4 (as illustrated by the diurnal profile in Fig. 2). The correlation is moderate ($r = 0.56$) when considering hourly concentrations, but is slightly higher with daily values ($r = 0.68$).

Several uncertainties may explain the discrepancies between observed and simulated HNO_3 concentrations: (i) uncertainties in NO_x emissions at both local and regional scales, (ii) uncertainties in the thermodynamic equilibrium (i.e. the errors on either the other inorganic compounds or the ISORROPIA model itself) that determines the distribution between gas and aerosol phases, (iii) uncertainties in the OH concen-

ACPD
15, 23731–23794, 2015

trations that directly influence the conversion of NO_2 into HNO_3, (iv) uncertainties on the nitric acid deposition, and (v) errors in the transport. At a European scale, uncertainties on NO_x emissions are estimated to be around 30 % (Deguillaume et al., 2007; Konovalov et al., 2006) and are thus much lower than the errors obtained for modelled HNO_3. Over the Paris agglomeration, NO_x emissions from the TNO-MP inventory used in our model have been evaluated during the summer 2009 based on aircraft measurements in the Paris plume, showing no significant bias (Petetin et al., 2014). Dry deposition plays an important role in the HNO_3 budget, and corresponding parameterizations incorporated in the CHIMERE model have been poorly evaluated so far. In fact, a too low deposition rate modelled by CHIMERE may partly explain the positive bias on HNO_3, but due to a lack of appropriate data, this hypothesis remains difficult to assess. Finally, important errors on the transport pattern remains unlikely given the good correlations obtained on nitrates between the observations and the model. The next subsections aim to investigate in more details the uncertainties related to simulated thermodynamic equilibrium and OH radical.

Uncertainties associated with thermodynamic equilibrium

Bias and quadratic error are much lower for total nitrate (NMB of +71 %, NRMSE of 121 %) than for HNO_3, because the CHIMERE model overestimates the fraction of gaseous nitric acid in TNO_3 (on average 68 % for the model against 51 % observed from experimental data during the period with available observations of NO_3 and HNO_3). Partitioning errors may derive from uncertainties in the ISORROPIA thermodynamic model (e.g. model formulation, chemical compounds included, activity coefficients treatment). Apart from CHIMERE, the ISORROPIA model is used in many other CTMs, including LOTOS-EUROS (Schaap et al., 2008), REM-CALGRID (Stern, 2003), CAMx, FARM or CMAQ. It has been validated in various studies based on comparisons with observations (Moya et al., 2001) or against other widely used thermodynamic models (Nenes et al., 1999; Carnevale et al., 2012) from which several uncertainty sources emerge. These uncertainties are introduced by the hypothesis (used in

ACPD
15, 23731–23794, 2015

ISORROPIA) of an instantaneous equilibrium between gas and aerosol phases (Aan de Brugh et al., 2012). However, such uncertainties are not expected here since the CHIMERE model treats the evolution of inorganic compounds concentrations through a dynamic approach (see Sect. 3.1). The absence of sodium, chloride and other crustal species (Ca^{2+}, K^{+}, Mg^{2+}) in our simulations may also induce errors in the system (Fountoukis and Nenes, 2007), but the contribution of this crustal material remains low in the Paris region, about 5 % on average from 1 April to 10 September (with a percentile 95 at 13 %), as previously noted by Bressi et al. (2013). This poor contribution of crustal species is confirmed by the ion balance obtained by considering only ammonium, nitrate and sulfate: NH_4^+ vs. $NO_3^- + 2SO_4^{2-}$ (all species expressed in neq m^{-3}) gives a slope of 1.01, an y intercept of −0.20 and a correlation $r^2 = 0.97$ (see Fig. S1 in the Supplement).

Therefore, errors in the modelled partitioning are most likely due to errors in the other inorganic compounds involved in the HNO_3-nitrate equilibrium. In particular, the large negative bias on NH_3 described in Sect. 4.2 can potentially lead to an underestimation of the ammonium nitrate formation and consequently to an overestimation of HNO_3. A sensitivity test has been performed for that purpose with the ISORROPIA model running alone (i.e. not coupled with CHIMERE) fed by the concentrations previously obtained with CHIMERE for inorganic species except for NH_3 for which measurements were taken into account. This approach changes HNO_3 concentrations, with for instance a decrease of 29 % in May. However, the significant positive bias in HNO_3 in summer persists (HNO_3 concentrations decrease by only 11 % between June and August). As a result, the misrepresentation of ammonia in the model (whose errors are maximum in early summer) cannot explain errors on modelled HNO_3 since TNO_3 is mostly related to HNO_3 due to high temperatures.

ACPD
15, 23731–23794, 2015

Uncertainties associated with OH concentrations

Assuming that (i) ($NO_2 + OH$) is likely the dominant direct homogeneous pathway for HNO_3 formation during the summertime period, (ii) a significant bias is observed for modelled TNO_3, and (iii) the maximum discrepancies between measurements and modelled HNO_3 are observed during mid-day, uncertainties on simulated OH could explain a substantial part of the errors on HNO_3. Many studies have attempted to quantify uncertainties on sources and sinks of OH, traditionally through the direct comparison between observations and calculations from detailed chemistry schemes (in box models) fed by ancillary observations of various parameters (e.g. VOC, NO_x and O_3 concentrations, photolysis rates). In such exercises, uncertainties on daytime OH concentrations usually remain below a factor of two (see Kanaya et al. (2007) for a review, where simulated over observed OH daytime concentrations ratios range between 0.5 and 1.5). During summertime, Michoud et al. (2012) have shown a very low overestimation (5 %) of OH concentrations simulated in Paris with the Master Chemical Mechanism (MCM) chemistry scheme. However, these results need to be taken as a lower end of OH uncertainties in CTMs where constraints are neither applied on long-lived compounds nor on photolysis rates. This is especially true in an urban environment where concentration gradients of compounds impacting on the OH budget are strong.

In order to assess the influence of OH on HNO_3 formation, a sensitivity test "MOD-OHx0.5" has been performed (over a period of 35 days in June/early July) by artificially reducing OH concentrations. This is done by decreasing by a factor of two the HO_x ($HO_x = OH + HO_2 + RO_2$) formation yields (i.e. the stoechiometric coefficient) in several (initiation) reactions, including the photolytic destruction of ozone, formaldehyde, acetaldehyde, glyoxal and methyl glyoxal. OH and HNO_3 concentrations are then compared with the reference MOD case in Fig. 10. On average, concentrations of both species are reduced by −36 and −16 %, respectively while changes in NO_x concentrations remain below 3 % (i.e. only a minor NO_x fraction is oxidized within Paris). These decreases are even more important during mid-day where it reaches −42 and −25 %,

ACPD
15, 23731–23794, 2015

respectively. Over mid-day, the bias between measured and modelled HNO_3 is reduced and equals to +113 % (against +154 % in the MOD case). Uncertainties in the OH radical may thus explain a significant part of the CHIMERE errors on nitric acid.

Local vs. advected contributions in CHIMERE

As mentioned in Sect. 4.3.1, differences between MOD and MOD-noIDF scenarios can be used to infer the contribution of local emissions (Paris city). However, as inorganic compounds are governed by non-linear processes (e.g. thermodynamics, chemistry), removing NO_x emissions over the Paris agglomeration may shift the equilibrium of HNO_3-NO_3^- system toward the gas phase, leading to an erroneous estimation of local and advected contributions of HNO_3. It thus appears more appropriate to consider here differences for TNO_3 which is not directly affected by equilibrium changes like HNO_3. A large part of TNO_3 simulated in the city is originated from outside the Paris region (77 % on a daily average for the whole campaign), even in summer (67 % from June to August) when TNO_3 remains mostly in the gas phase (i.e. HNO_3). This contribution varies from 68 % in the afternoon to more than 90 % during the night. As illustrated in Fig. 11, a clear south-to-north gradient appears over the MED domain, with the highest TNO_3 concentrations simulated over North of France, Belgium and the Netherlands, in the vicinity of high NO_x emissions. This result may underline a low contribution of local NO_x emissions which was not expected given their intensity in the Paris agglomeration (like the unexpected low contribution of primary traffic emissions to nitrates in Paris found by Bressi et al., 2014). Such low contribution of local TNO_3 formation in the model could be explained by the dispersive conditions (flat terrain) met in Paris and its surrounding regions and the time scale of NO_x-to-HNO_3 conversion (around a few hours) which favors nitric acid production in the Paris plume rather than within the city (despite the possible overestimation of OH concentrations).

On the other hand, according to the CHIMERE model, most of the highest HNO_3 episodes shown in Fig. 5b are associated to a rather similar contribution between local formation vs. import (the contribution of import ranging from 40 to 60 % depending

ACPD
15, 23731–23794, 2015

on the day), except the 5 and 30 June that are mainly associated with local pattern (with import contributing to 30 and 23 %, respectively) and the 19 April that is essentially driven by import (90 %). However, given the high errors on the simulation of HNO_3 concentrations in Paris, it is difficult to assess the reliability of the obtained relative contributions, and uncertainties must be reduced before drawing a more detailed picture of the geographical budget of nitric acid.

4.3.3 Conclusions on HNO_3

Nitric acid concentrations experimentally determined in Paris show several intense peaks in late spring and early summer that coincide with high air temperatures and low to moderate winds. The share between local production and imports remains difficult to assess precisely, but analysis results suggest that the contribution of imports may be substancial, if not dominant, on average while local HNO_3 may represent a major source on more specific time-limited episodes. However, uncertainties persist, and the CHIMERE errors are unfortunately too high to help the investigation of HNO_3 origin. Indeed, the model largely overestimates measured HNO_3 concentrations, approximately by a factor 3, with the highest biases observed in the middle of the day. The negative bias between measured and modelled NH_3 explains a part of the poor model performance for HNO_3, but still fails to explain errors during summertime when TNO_3 is mostly related to HNO_3. Uncertainties on NO_x emissions are much lower than errors obtained on HNO_3 and cannot explain the results of the model. Uncertainties related to the dry deposition of HNO_3 could not be assessed and could contribute to the discrepancies given by the model. Finally, a too strong NO_2-to-HNO_3 conversion through an overestimation of the OH radical concentrations in CHIMERE could also contribute to the large modelled overestimation of HNO_3 formation. Indeed, uncertainties on simulated OH remain still high in CTMs, probably more than a factor of 2, and reducing OH sources have shown to lead to a significant decrease of OH and HNO_3 concentrations, in particular during the afternoon when NO_2 photooxidation is at its maximum.

ACPD
15, 23731–23794, 2015

4.4 Aerosol nitrate formation

4.4.1 Results of the CHIMERE simulations

Fine particulate pollution with high nitrate contents in Paris consists in intense (up to 16 $\mu g\,m^{-3}$ in late spring) and time-limited (a few days) episodes associated with continental wind regimes. Very low levels of nitrate are observed during periods with marine (clean) air masses and during summertime (due to volatilization). Despite the large errors reported by the model in the previous sections for both NH_3 and HNO_3, the CHIMERE model provides quite satisfactory results for nitrate with a mean bias of +19 % and a correlation of 0.81, but still with a large NRMSE (109 %). However, this positive bias should partly originate from experimental (negative) artifacts and actually, the model may underestimate the nitrate concentrations if the experimental data are corrected for semi-volatile losses. Indeed, if we attribute all the semi-volatile particulate matter deduced from the difference between TEOM-FDMS and TEOM $PM_{2.5}$ concentrations to ammonium nitrate (which is not fully correct since semi-volatile OA may also contribute to this semi-volatile particulate matter), the bias between measured and modelled nitrates is −48 %. Indeed, the correlation between this semi-volatile matter and the OA measured during the campaign is much higher than with ammonium nitrate (0.59 against 0.32), which suggests that a noticeable part of these losses is OA. As a conclusion, the either positive or negative bias on simulated nitrate remains small, despite significant biases reported previously for precursor species. It would be useful in the near future to evaluate the CHIMERE model with artefact-free measurements (for instance with aerosol mass spectrometer (AMS) or aerosol chemical speciation monitor (ACSM)).

4.4.2 Gas Ratio and limited species for nitrate formation

The Gas Ratio (GR) has been proposed to assess which species among ammonia and nitric acid is the limiting reactant for ammonium nitrate formation (Ansari and Pandis,

ACPD
15, 23731–23794, 2015

1998). It is defined as follows (with concentrations expressed in ppb):

$$GR = \frac{[TNH_3] - 2\left[SO_4^{2-}\right]}{[TNO_3]} \quad (6)$$

GR values above 1 indicate a regime mainly limited by nitric acid (i.e. NH_3-rich regime) in which there is enough NH_3 to neutralize both sulfate and nitrate. Conversely, a GR between 0 and 1 indicates that there is enough NH_3 to neutralize sulfate but not nitrate, while negative GR correspond to a NH_3-poor regime in which NH_3 amounts are insufficient to even neutralize sulfate. Non-linear PM responses to inorganic concentration changes are expected at GR near unity (Ansari and Pandis, 1998).

As shown on Fig. 12, daily GR measurements are available only from the end of May (no NH_3 observations before) until the beginning of September (no aerosol observations after). During that period, experimentally determined daily GR values are highly variable (ranging between 2.8 to 56.3) but always remain above unity (12.6 on average), thus indicating that a large amount of ammonia is available for neutralizing nitric acid.

By definition, GR does not depend on the partitioning of TNH_3 and TNO_3, and thus should not be influenced by potential artefacts related to this partitioning. However, in our case, NH_3 and NH_4^+ (as well as HNO_3 and NO_3^-) are not measured by the same instrument (nor even at the same site), and the evaporated ammonium for instance cannot be found in the NH_3 measurement. Thus, observed GR may be overestimated due to the negative artefacts of nitrate filter measurements (Sect. 2.1). If we assume here that all that lost semi-volatile material (deduced from the discrepancies between TEOM-FDMS and gravimetric measurements) is ammonium nitrate, one can calculate an artefact-corrected GR with both evaporated ammonium and nitrate added to measured TNH_3 and TNO_3, respectively. Compared to the previous GR, the artefact-corrected GR is reduced to an average value of 7.3 (the median is 3.5), thus still well above 1. In addition, as noticeable amounts of organic matter are expected to be included in the evaporated part, this artefact-corrected GR has to be considered

ACPD
15, 23731–23794, 2015

as a lower estimate of the actual GR values. The nitrate formation in Paris thus appears mainly limited by nitric acid. Over Europe, Pay et al. (2012) have also observed GR above 1 in several regions (e.g. Switzerland, Italy, Austria, inland regions of Spain and Denmark; no data in France), but taking into account observations restricted to regional background stations (i.e. enriched by agriculture (NH_3) emissions instead of traffic (NO_x) emissions). In our study, we show that such a NH_3-rich regime is also observed for a large megacity like Paris. Considering the high NO_x emissions in the Paris megacity, such a result is very interesting, but could likely be explained, as previously mentioned in Sect. 4.3.2, by a too slow NO_x-to-HNO_3 conversion rate compared to the efficient dispersive conditions.

In the CHIMERE model, the negative bias on TNH_3 and the positive ones on TNO_3 and SO_4^{2-} concur of all them to a significant underestimation of modelled GR. On average, the model simulates a GR slightly above unity (1.2). Daily values continuously alternate between both regimes with, over the period with available observations data (100 days), 48 % of simulated daily values remaining below unity (47 % considering the whole dataset). The dataset does not show any period with specific (and permanent) pattern for GR. Actually, the diurnal profile given by CHIMERE indicates that the regime changes within a single day, the lowest GR values (below 1) being simulated at 12:00 UTC (between the maximum TNO_3 occurring at 08:00 UTC and the minimum TNH_3 simulated at 15:00 UTC). Therefore, due to significant errors in gaseous precursors (and to a lesser extent in sulfate), the CHIMERE model fails half of time at retrieving correctly the HNO_3-limited regime for nitrate formation in Paris on a daily basis.

4.4.3 Sensitivity to perturbations

The GR alone does not allow predicting the sensitivity of nitrate formation with respect to changes in gas precursors concentrations. This is due to the inability of GR to take into account neither the need for the atmosphere to be saturated with NH_3 and HNO_3 (which acts as a threshold effect), nor the influence of temperature and RH.

ACPD
15, 23731–23794, 2015

Additional information can be given by the sensitivity coefficient S_x (Takahama et al., 2004) to nitrate formation, defined as:

$$S_x = \frac{\Delta NO_3}{NO_3} \frac{x}{\Delta x} \quad (7)$$

where ΔNO_3 refers to the change in nitrate concentrations obtained after a Δx change of the parameter x (e.g. temperature, RH, TNH_3, TNO_3 or TS).

The ISORROPIA thermodynamic model is used here to compute this sensitivity coefficient S_x as a function of various decreases (−10, −25, −50 and −90 %) in TNH_3 and TNO_3 concentrations. Calculations are performed for both the measurements and the model. Sensitivity coefficient results and corresponding GR are shown as box plots in Fig. 13.

For the experimental data, we do observe a quite similar sensitivity of nitrate formation for changes either in TNH_3 or in TNO_3 concentrations, with median sensitivity coefficients around 1 (i.e. close to a linear response). Considering the high GR values (except for the −50 and −90 % TNH_3 cases that lead to negative GR), such a result with similar responses to both precursors changes appears quite counter-intuitive in light of the above definition of GR. First, the GR approach considers free NH_3, while the sensitivities are calculated with respect to total NH_3. Second, the nitrate formation is possible only if the saturation condition is achieved (Ansari and Pandis, 1998):

$$[TNO_3] \cdot ([TNH_3] - 2[TS]) > K \quad (8)$$

with K the equilibrium constant. So for large GR values, but small TNO_3 and free NH_3 values, nitrate formation will be sensitive to both TNO_3 and TNH_3. Note that K (and thus the nitrate sensitivity) also depends on temperature and RH; this is illustrated in Fig. S6 in the Supplement where the same sensitivity tests are performed after decreasing the temperature by 10 °C and increasing the RH by 0.20 in observations, which leads to S_{TNO_3} (still close to 1) much higher than S_{TNH_3} (below 0.5 for −10 and −25 % of TNH_3), in accordance with the NH_3-rich regime given by GR.

ACPD
15, 23731–23794, 2015

The CHIMERE nitrate response to TNO_3 changes is approximately linear (i.e. S_{TNO_3} close to 1), in reasonable agreement with observations. However, the model highly overestimates the sensitivity to TNH_3 changes, with median S_{TNH_3} up to 2.5 for moderate NH_3 decreases while observations show a similar response than for TNO_3 changes (S_{TNH_3} around 1). The model manages to match the observed response only when nitrate formation is severely NH_3 limited (negative GR) and when the aerosol nitrate formation is prevented (which corresponds to the −90 % TNH_3 case).

These results have serious implications on the use of the CHIMERE model for emissions reduction scenarios. As TNH_3 concentrations are closely linked to NH_3 emissions, they show that the benefits (in terms of fine aerosol concentrations) of reducing these emissions would likely be overestimated by the model, in particular for moderate reductions (below −50 %). In addition, in terms of dynamical evaluation, changes in NH_3 emissions in the next years may potentially degrade the CHIMERE performance on the simulation of ammonium nitrates in Paris if the issues raised here are not solved. This is an important conclusion for the use of the CHIMERE model (in that configuration and input data) and probably other CTMs sharing similar input data and/or parameterizations.

5 Conclusions

Ammonium nitrate is a major contributor to the fine particulate pollution in Europe, and a better characterization of its formation regime and variability (controlled by the availability of its gaseous precursors, ammonia and nitric acid) is thus mandatory for setting up relevant PM control strategies.

In this study, long term measurements of inorganic compounds in both gaseous (NH_3, HNO_3, SO_2) and aerosol (NH_4^+, NO_3^-, SO_4^{2-}) fractions have been used to assess the nitrate formation regime in the Paris megacity over several months covering the spring/summer period. High episodes of ammonia (up to 12 ppb on daily average) were observed during late spring and early summer suggesting sources related to agri-

ACPD
15, 23731–23794, 2015

culture activities. Rather low nitric acid concentrations were measured (below 1.5 ppb on daily average), despite the large amounts of gas precursors (NO_x) emitted by traffic emissions in the city of Paris. Observations made on NH_3 and HNO_3 indicate that wind regimes in Paris are sufficient to allow significant NH_3 imports from outside the agglomeration and to prevent local formation of nitric acid. These experimental results lead to a NH_3-rich regime in the Paris urban environment (as indicated by high gas ratio values), as already observed in previous studies over Europe but only in rural areas (i.e. closer to agricultural activities). However, sensitivity tests with the ISORROPIA thermodynamic model indicate that, in the specific environment of Paris (in terms of relative humidity, temperature and inorganic compounds concentrations), the nitrate formation remains quite equally influenced by decreases of TNH_3 and TNO_3. This work thus sheds a new light on the topical debate relative to the respective responsibility of trafic and agriculture in the formation of ammonium nitrate.

This detailed experimental dataset has also offered the opportunity to evaluate the ability of the CHIMERE chemistry-transport model to simulate the NH_3-HNO_3-NO_3^- system. Comparison between measurements and model have shown significant negative (−75 %) and positive (+195 %) biases for ammonia and nitric acid, respectively. Several sensitivity tests have been performed in order to rank uncertainty sources being responsible for these important biases. The difficulty of the CHIMERE model to match ammonia observations is likely mainly due to erroneous agricultural emissions. By comparison, the contribution of NH_3 traffic emissions in the Paris agglomeration appears as minor during the studied period but requires a more detailed quantification. Besides the (hardly quantifiable) uncertainties associated with dry deposition, errors on nitric acid can probably be explained by the large uncertainties on OH concentrations, in particular during summertime while the negative bias on ammonia explains a significant part of the nitric acid overestimation during spring (by preventing HNO_3 to be converted into nitrate).

Many studies have evaluated the ability of CTMs to simulate inorganic aerosol compounds, but very few have evaluated their performances on gaseous precursors. The

ACPD
15, 23731–23794, 2015

low performing modelled results on nitric acid and ammonia found here may also exist in other CTMs sharing similar emissions data and/or parameterizations. The sensitivity of nitrate formation as a function of decreasing concentrations of gas precursor have been investigated, highlighting a very high sensitivity to NH_3 changes in the model, in disagreement with observations that give a quasi linear response. Such results may have important implications on the use of CHIMERE for emission reduction scenarios (at least in the Paris region) by potentially overestimating the potential benefit of NH_3 emission reductions in terms of PM concentrations. The diagnostic evaluation led in this paper gives first results that need to be extended, notably with hourly artefact-free (ammonium nitrate) measurements during all seasons, in order to assess more precisely the nitrate formation regime in the city of Paris. Additional work on uncertainty sources is also required to reduce the highlighted errors, in particular the NH_3 agricultural emissions and the OH uncertainties. In that perspectives, the recent NH_3 measurements provided by IASI (Infrared Atmospheric Sounding Interferometer; Clarisse et al., 2009, 2010) may offer opportunities to better assess the spatial distribution of NH_3 emissions and help building more accurate emission inventories.

The Supplement related to this article is available online at doi:10.5194/acpd-15-23731-2015-supplement.

Acknowledgements. This work is funded by a PhD DIM (*domaine d'intérêt majeur*) grant from the Ile-de-France region. The PARTICULES project has been funded by the French state, the Ile-de-France region and the Paris city. The FRANCIPOL projet has received funding from PRIMEQUAL, CNRS, CEA, the Ile-de-France region, ACTRIS and DIM R2DS. The authors gratefully acknowledge Jean-Charles Dupont and the SIRTA (sirta.ipsl.fr) for the useful boundary layer height data. The other meteorological data at Montsouris site have been kindly provided by METEO France.

ACPD
15, 23731–23794, 2015

References

Aan de Brugh, J. M. J., Henzing, J. S., Schaap, M., Morgan, W. T., van Heerwaarden, C. C., Weijers, E. P., Coe, H., and Krol, M. C.: Modelling the partitioning of ammonium nitrate in the convective boundary layer, Atmos. Chem. Phys., 12, 3005–3023, doi:10.5194/acp-12-3005-2012, 2012.

Airparif: Inventaire des émissions en Ile-de-France en 2005, available at: http://www.airparif.asso.fr/_pdf/publications/Rinventaire_2005_201004.pdf (last access: 12 June 2015), 2010.

Airparif: Origine des particules en Ile-de-France, available at: http://www.airparif.asso.fr/_pdf/publications/rapport-particules-110914.pdf (last access: 12 June 2015), 2011.

Airparif: Source apportionment of airborne particles in the Ile-de-France region, available at: http://www.airparif.asso.fr/_pdf/publications/rapport-particules-anglais-120829.pdf (last access: 12 June 2015), 2012.

Ansari, A. S. and Pandis, S. N.: Response of inorganic PM to precursor concentrations, Environ. Sci. Technol., 32, 2706–2714, doi:10.1021/es971130j, 1998.

Asman, W. A. H., Sutton, M. A., and Schjorring, J. K.: Ammonia: emission, atmospheric transport and deposition, New Phytol., 139, 27–48, doi:10.1046/j.1469-8137.1998.00180.x, 1998.

Baklanov, A., Lawrence, M., Pandis, S., Mahura, A., Finardi, S., Moussiopoulos, N., Beekmann, M., Laj, P., Gomes, L., Jaffrezo, J.-L., Borbon, A., Coll, I., Gros, V., Sciare, J., Kukkonen, J., Galmarini, S., Giorgi, F., Grimmond, S., Esau, I., Stohl, A., Denby, B., Wagner, T., Butler, T., Baltensperger, U., Builtjes, P., van den Hout, D., van der Gon, H. D., Collins, B., Schluenzen, H., Kulmala, M., Zilitinkevich, S., Sokhi, R., Friedrich, R., Theloke, J., Kummer, U., Jalkinen, L., Halenka, T., Wiedensholer, A., Pyle, J., and Rossow, W. B.: MEGAPOLI: concept of multi-scale modelling of megacity impact on air quality and climate, Adv. Sci. Res., 4, 115–120, doi:10.5194/asr-4-115-2010, 2010.

Behera, S. N., Betha, R., and Balasubramanian, R.: Insights into chemical coupling among acidic gases, ammonia and secondary inorganic aerosols, Aerosol Air Qual. Res., 13, 1282–1296, doi:10.4209/aaqr.2012.11.0328, 2013.

Bessagnet, B., Menut, L., Curci, G., Hodzic, A., Guillaume, B., Liousse, C., Moukhtar, S., Pun, B., Seigneur, C., and Schulz, M.: Regional modeling of carbonaceous aerosols over Europe – focus on secondary organic aerosols, J. Atmos. Chem., 61, 175–202, doi:10.1007/s10874-009-9129-2, 2009.

ACPD
15, 23731–23794, 2015

Bishop, G. A., Peddle, A. M., Stedman, D. H., and Zhan, T.: On-road emission measurements of reactive nitrogen compounds from three California cities, Environ. Sci. Technol., 44, 3616–3620, doi:10.1021/es903722p, 2010.

Blanchard, C. L. and Hidy, G. M.: Effects of changes in sulfate, ammonia, and nitric acid on particulate nitrate concentrations in the Southeastern United States, J. Air Waste Manage., 53, 283–290, doi:10.1080/10473289.2003.10466152, 2003.

Bressi, M., Sciare, J., Ghersi, V., Bonnaire, N., Nicolas, J. B., Petit, J.-E., Moukhtar, S., Rosso, A., Mihalopoulos, N., and Féron, A.: A one-year comprehensive chemical characterisation of fine aerosol ($PM_{2.5}$) at urban, suburban and rural background sites in the region of Paris (France), Atmos. Chem. Phys., 13, 7825–7844, doi:10.5194/acp-13-7825-2013, 2013.

Bressi, M., Sciare, J., Ghersi, V., Mihalopoulos, N., Petit, J.-E., Nicolas, J. B., Moukhtar, S., Rosso, A., Féron, A., Bonnaire, N., Poulakis, E., and Theodosi, C.: Sources and geographical origins of fine aerosols in Paris (France), Atmos. Chem. Phys., 14, 8813–8839, doi:10.5194/acp-14-8813-2014, 2014.

Cadle, S., Countess, R., and Kelly, N.: Nitric acid and ammonia in urban and rural locations, Atmos. Environ., 16, 2501–2506, doi:10.1016/0004-6981(82)90141-X, 1982.

Cadle, S. H.: Seasonal variations in nitric acid, nitrate, strong aerosol acidity, and ammonia in an urban area, Atmos. Environ., 19, 181–188, doi:10.1016/0004-6981(85)90149-0, 1985.

Camargo, J. A. and Alonso, A.: Ecological and toxicological effects of inorganic nitrogen pollution in aquatic ecosystems: a global assessment, Environ. Int., 32, 831–849, doi:10.1016/j.envint.2006.05.002, 2006.

Carnevale, C., Finzi, G., Pisoni, E., Thunis, P., and Volta, M.: The impact of thermodynamic module in the CTM performances, Atmos. Environ., 61, 652–660, doi:10.1016/j.atmosenv.2012.06.058, 2012.

Carslaw, D. C. and Rhys-Tyler, G.: New insights from comprehensive on-road measurements of NO_x, NO_2 and NH_3 from vehicle emission remote sensing in London, UK, Atmos. Environ., 81, 339–347, doi:10.1016/j.atmosenv.2013.09.026, 2013.

Chow, J. C.: Health effects of fine particulate air pollution: lines that connect, J. Air Waste Manage., 56, 707–708, doi:10.1080/10473289.2006.10464484, 2006.

CITEPA: Inventaire des émissions de polluants atmosphériques et de gaz à effet de serre en France – Séries sectorielles et analyses étendues, 2013.

ACPD
15, 23731–23794, 2015

Clarisse, L., Clerbaux, C., Dentener, F., Hurtmans, D., and Coheur, P.-F.: Global ammonia distribution derived from infrared satellite observations, Nat. Geosci., 2, 479–483, doi:10.1038/ngeo551, 2009.

Clarisse, L., Shephard, M. W., Dentener, F., Hurtmans, D., Cady-Pereira, K., Karagulian, F., Van Damme, M., Clerbaux, C., and Coheur, P.-F.: Satellite monitoring of ammonia: a case study of the San Joaquin Valley, J. Geophys. Res., 115, D13302, doi:10.1029/2009JD013291, 2010.

Dall'Osto, M., Harrison, R. M., Coe, H., and Williams, P.: Real-time secondary aerosol formation during a fog event in London, Atmos. Chem. Phys., 9, 2459–2469, doi:10.5194/acp-9-2459-2009, 2009.

Davidson, C. I. and Wu, Y. L.: Dry deposition of particle and vapors, in: Acidic Precipitation, edited by: Lindberg, S. E., Page, A. L., and Norton, S. A., vol. 3, Springer Verlag, New York, 103–216, 1990.

Deguillaume, L., Beekmann, M., and Menut, L.: Bayesian Monte Carlo analysis applied to regional-scale inverse emission modeling for reactive trace gases, J. Geophys. Res., 112, D02307, doi:10.1029/2006JD007518, 2007.

Ellis, R. A., Murphy, J. G., Markovic, M. Z., VandenBoer, T. C., Makar, P. A., Brook, J., and Mihele, C.: The influence of gas-particle partitioning and surface-atmosphere exchange on ammonia during BAQS-Met, Atmos. Chem. Phys., 11, 133–145, doi:10.5194/acp-11-133-2011, 2011.

Erisman, J. W., Otjes, R., Hensen, A., Jongejan, P., van den Bulk, P., Khlystov, A., Möls, H., and Slanina, S.: Instrument development and application in studies and monitoring of ambient ammonia, Atmos. Environ., 35, 1913–1922, doi:10.1016/S1352-2310(00)00544-6, 2001.

Favez, O., Cachier, H., Sciare, J., and Le Moullec, Y.: Characterization and contribution to $PM_{2.5}$ of semi-volatile aerosols in Paris (France), Atmos. Environ., 41, 7969–7976, doi:10.1016/j.atmosenv.2007.09.031, 2007.

Folberth, G. A., Hauglustaine, D. A., Lathière, J., and Brocheton, F.: Interactive chemistry in the Laboratoire de Météorologie Dynamique general circulation model: model description and impact analysis of biogenic hydrocarbons on tropospheric chemistry, Atmos. Chem. Phys., 6, 2273–2319, doi:10.5194/acp-6-2273-2006, 2006.

Fountoukis, C. and Nenes, A.: ISORROPIA II: a computationally efficient thermodynamic equilibrium model for K^+–Ca^{2+}–Mg^{2+}–NH_4^+–Na^+–SO_4^{2-}–NO_3^-–Cl^-–H_2O aerosols, Atmos. Chem. Phys., 7, 4639–4659, doi:10.5194/acp-7-4639-2007, 2007.

ACPD
15, 23731–23794, 2015

Garcia, L., Bedos, C., Génermont, S., Braud, I., and Cellier, P.: Assessing the ability of mechanistic volatilization models to simulate soil surface conditions: a study with the Volt'Air model, Sci. Total Environ., 409, 3980–3992, doi:10.1016/j.scitotenv.2011.05.003, 2011.

Génermont, S. and Cellier, P.: A mechanistic model for estimating ammonia volatilization from slurry applied to bare soil, Agr. Forest Meteorol., 88, 145–167, doi:10.1016/S0168-1923(97)00044-0, 1997.

Grantz, D. A., Garner, J. H. B., and Johnson, D. W.: Ecological effects of particulate matter, Environ. Int., 29, 213–239, doi:10.1016/S0160-4120(02)00181-2, 2003.

Guenther, A., Karl, T., Harley, P., Wiedinmyer, C., Palmer, P. I., and Geron, C.: Estimates of global terrestrial isoprene emissions using MEGAN (Model of Emissions of Gases and Aerosols from Nature), Atmos. Chem. Phys., 6, 3181–3210, doi:10.5194/acp-6-3181-2006, 2006.

Haeffelin, M., Angelini, F., Morille, Y., Martucci, G., Frey, S., Gobbi, G. P., Lolli, S., O'Dowd, C. D., Sauvage, L., Xueref-Rémy, I., Wastine, B., and Feist, D. G.: Evaluation of mixing-height retrievals from automatic profiling lidars and ceilometers in view of future integrated networks in Europe, Bound.-Lay. Meteorol., 143, 49–75, doi:10.1007/s10546-011-9643-z, 2011.

Hamaoui-Laguel, L., Meleux, F., Beekmann, M., Bessagnet, B., Génermont, S., Cellier, P., and Létinois, L.: Improving ammonia emissions in air quality modelling for France, Atmos. Environ., 92, 584–595, doi:10.1016/j.atmosenv.2012.08.002, 2014.

Hansen, M. C., Defries, R. S., Townshend, J. R. G., and Sohlberg, R.: Global land cover classification at 1 km spatial resolution using a classification tree approach, Int. J. Remote Sens., 21, 1331–1364, doi:10.1080/014311600210209, 2000.

Harrison, R. M. and Pio, C. A.: Size-differentiated composition of inorganic atmospheric aerosols of both marine and polluted continental origin, Atmos. Environ., 17, 1733–1738, doi:10.1016/0004-6981(83)90180-4, 1983.

Hass, H., Van Loon, M., Kessler, C., Stern, R., Matthijsen, J., Sauter, F., Zlatev, Z., Langner, J., Foltescu, V., and Schaap, M.: Aerosol modelling: results and intercomparison from European regional scale modeling systems, A contribution to the EUROTRAC-2 subproject GLOREAM, EUROTRAC report, 2003.

Hauglustaine, D. A.: Interactive chemistry in the Laboratoire de Météorologie Dynamique general circulation model: description and background tropospheric chemistry evaluation, J. Geophys. Res., 109, D04314, doi:10.1029/2003JD003957, 2004.

ACPD
15, 23731–23794, 2015

Healy, R. M., Sciare, J., Poulain, L., Kamili, K., Merkel, M., Müller, T., Wiedensohler, A., Eckhardt, S., Stohl, A., Sarda-Estève, R., McGillicuddy, E., O'Connor, I. P., Sodeau, J. R., and Wenger, J. C.: Sources and mixing state of size-resolved elemental carbon particles in a European megacity: Paris, Atmos. Chem. Phys., 12, 1681–1700, doi:10.5194/acp-12-1681-2012, 2012.

IPCC: Climate Change 2013: the Physical Science Basis, available at: http://www.ipcc.ch/report/ar5/wg1/ (last access: 12 June 2015), 2013.

Kanaya, Y., Cao, R., Akimoto, H., Fukuda, M., Komazaki, Y., Yokouchi, Y., Koike, M., Tanimoto, H., Takegawa, N., and Kondo, Y.: Urban photochemistry in central Tokyo: 1. Observed and modeled OH and HO_2 radical concentrations during the winter and summer of 2004, J. Geophys. Res., 112, D21312, doi:10.1029/2007JD008670, 2007.

Kean, A. J., Littlejohn, D., Ban-Weiss, G. A., Harley, R. A., Kirchstetter, T. W., and Lunden, M. M.: Trends in on-road vehicle emissions of ammonia, Atmos. Environ., 43, 1565–1570, doi:10.1016/j.atmosenv.2008.09.085, 2009.

Kim, Y., Couvidat, F., Sartelet, K., and Seigneur, C.: Comparison of different gas-phase mechanisms and aerosol modules for simulating particulate matter formation, J. Air Waste Manage., 61, 1218–1226, 2011.

Konovalov, I. B., Beekmann, M., Richter, A., and Burrows, J. P.: Inverse modelling of the spatial distribution of NO_x emissions on a continental scale using satellite data, Atmos. Chem. Phys., 6, 1747–1770, doi:10.5194/acp-6-1747-2006, 2006.

Kuenen, J., Denier van der Gon, H. A. C., Visschedijk, A., van der Brugh, H., and van Gijlswijk, R.: MACC European emission inventory for the years 2003–2007, Tech. rep., TNO, 2011.

Kuenen, J. J. P., Visschedijk, A. J. H., Jozwicka, M., and Denier van der Gon, H. A. C.: TNO-MACC_II emission inventory; a multi-year (2003–2009) consistent high-resolution European emission inventory for air quality modelling, Atmos. Chem. Phys., 14, 10963–10976, doi:10.5194/acp-14-10963-2014, 2014.

Lombardo, T., Gentaz, L., Verney-Carron, A., Chabas, A., Loisel, C., Neff, D., and Leroy, E.: Characterisation of complex alteration layers in medieval glasses, Corros. Sci., 72, 10–19, doi:10.1016/j.corsci.2013.02.004, 2013.

Ma, B. L., Wu, T. Y., Tremblay, N., Deen, W., McLaughlin, N. B., Morrison, M. J., and Stewart, G.: On-farm assessment of the amount and timing of nitrogen fertilizer on ammonia volatilization, Agron. J., 102, 134–144, doi:10.2134/agronj2009.0021, 2010.

ACPD
15, 23731–23794, 2015

Massad, R.-S., Nemitz, E., and Sutton, M. A.: Review and parameterisation of bi-directional ammonia exchange between vegetation and the atmosphere, Atmos. Chem. Phys., 10, 10359–10386, doi:10.5194/acp-10-10359-2010, 2010.

Mather, T. A., Allen, A. G., Davison, B. M., Pyle, D. M., Oppenheimer, C., and McGonigle, A. J. S.: Nitric acid from volcanoes, Earth Planet. Sc. Lett., 218, 17–30, doi:10.1016/S0012-821X(03)00640-X, 2004.

Matsumoto, K. and Tanaka, H.: Formation and dissociation of atmospheric particulate nitrate and chloride: an approach based on phase equilibrium, Atmos. Environ., 30, 639–648, doi:10.1016/1352-2310(95)00290-1, 1996.

Menut, L., Bessagnet, B., Khvorostyanov, D., Beekmann, M., Blond, N., Colette, A., Coll, I., Curci, G., Foret, G., Hodzic, A., Mailler, S., Meleux, F., Monge, J.-L., Pison, I., Siour, G., Turquety, S., Valari, M., Vautard, R., and Vivanco, M. G.: CHIMERE 2013: a model for regional atmospheric composition modelling, Geosci. Model Dev., 6, 981–1028, doi:10.5194/gmd-6-981-2013, 2013.

Michoud, V., Kukui, A., Camredon, M., Colomb, A., Borbon, A., Miet, K., Aumont, B., Beekmann, M., Durand-Jolibois, R., Perrier, S., Zapf, P., Siour, G., Ait-Helal, W., Locoge, N., Sauvage, S., Afif, C., Gros, V., Furger, M., Ancellet, G., and Doussin, J. F.: Radical budget analysis in a suburban European site during the MEGAPOLI summer field campaign, Atmos. Chem. Phys., 12, 11951–11974, doi:10.5194/acp-12-11951-2012, 2012.

Moya, M., Ansari, A. S., and Pandis, S. N.: Partitioning of nitrate and ammonium between the gas and particulate phases during the 1997 IMADA-AVER study in Mexico City, Atmos. Environ., 35, 1791–1804, doi:10.1016/S1352-2310(00)00292-2, 2001.

Mozurkewich, M.: The dissociation constant of ammonium nitrate and its dependence on temperature, relative humidity and particle size, Atmos. Environ.-A Gen., 27, 261–270, doi:10.1016/0960-1686(93)90356-4, 1993.

Mulawa, P. A., Cadle, S. H., Lipari, F., Ang, C. C., and Vandervennet, R.: Urban dew: its composition and influence on dry deposition rates, Atmos. Environ., 20, 1389–1396, doi:10.1016/0004-6981(86)90009-0, 1986.

Nenes, A., Pandis, S. N., and Pilinis, C.: ISORROPIA?: a new thermodynamic equilibrium model for multiphase multicomponent inorganic aerosols, Aquat. Geochem., 4, 123–152, doi:10.1023/A:1009604003981, 1998.

ACPD
15, 23731–23794, 2015

Nenes, A., Pandis, S. N., and Pilinis, C.: Continued development and testing of a new thermodynamic aerosol module for urban and regional air quality models, Atmos. Environ., 33, 1553–1560, doi:10.1016/S1352-2310(98)00352-5, 1999.

Neuman, J. A., Huey, L. G., Ryerson, T. B., and Fahey, D. W.: Study of inlet materials for sampling atmospheric nitric acid, Environ. Sci. Technol., 33, 1133–1136, doi:10.1021/es980767f, 1999.

Nimmermark, S. and Gustafsson, G.: Influence of temperature, humidity and ventilation rate on the release of odour and ammonia in a floor housing system for laying hens, International commission of agricultural engineering, 2005.

Norman, M., Spirig, C., Wolff, V., Trebs, I., Flechard, C., Wisthaler, A., Schnitzhofer, R., Hansel, A., and Neftel, A.: Intercomparison of ammonia measurement techniques at an intensively managed grassland site (Oensingen, Switzerland), Atmos. Chem. Phys., 9, 2635–2645, doi:10.5194/acp-9-2635-2009, 2009.

Ottley, C. J. and Harrison, R. M.: The spatial distribution and particle size of some inorganic nitrogen, sulphur and chlorine species over the North Sea, Atmos. Environ.-A Gen., 26, 1689–1699, doi:10.1016/0960-1686(92)90067-U, 1992.

Pang, Y., Eatough, N. L., Wilson, J., and Eatough, D. J.: Effect of semivolatile material on $PM_{2.5}$ measurement by the $PM_{2.5}$ federal reference method sampler at Bakersfield, California, Aerosol Sci. Tech., 36, 289–299, doi:10.1080/027868202753504489, 2002.

Parmar, R., Satsangi, G., Lakhani, A., Srivastava, S., and Prakash, S.: Simultaneous measurements of ammonia and nitric acid in ambient air at Agra (27°10′ N and 78°05′ E) (India), Atmos. Environ., 35, 5979–5988, doi:10.1016/S1352-2310(00)00394-0, 2001.

Pay, M. T., Jiménez-Guerrero, P., and Baldasano, J. M.: Assessing sensitivity regimes of secondary inorganic aerosol formation in Europe with the CALIOPE-EU modeling system, Atmos. Environ., 51, 146–164, doi:10.1016/j.atmosenv.2012.01.027, 2012a.

Perrino, C., Catrambone, M., Di Menno Di Bucchianico, A., and Allegrini, I.: Gaseous ammonia in the urban area of Rome, Italy and its relationship with traffic emissions, Atmos. Environ., 36, 5385–5394, doi:10.1016/S1352-2310(02)00469-7, 2002.

Petetin, H., Beekmann, M., Sciare, J., Bressi, M., Rosso, A., Sanchez, O., and Ghersi, V.: A novel model evaluation approach focusing on local and advected contributions to urban $PM_{2.5}$ levels – application to Paris, France, Geosci. Model Dev., 7, 1483–1505, doi:10.5194/gmd-7-1483-2014, 2014.

ACPD
15, 23731–23794, 2015

Petit, J.-E., Favez, O., Sciare, J., Crenn, V., Sarda-Estève, R., Bonnaire, N., Močnik, G., Dupont, J.-C., Haeffelin, M., and Leoz-Garziandia, E.: Two years of near real-time chemical composition of submicron aerosols in the region of Paris using an Aerosol Chemical Speciation Monitor (ACSM) and a multi-wavelength Aethalometer, Atmos. Chem. Phys., 15, 2985–3005, doi:10.5194/acp-15-2985-2015, 2015.

Pierson, W. R., Brachaczek, W. W., Japar, S. M., Cass, G. R., and Solomon, P. A.: Dry deposition and dew chemistry in Claremont, California, during the 1985 nitrogen species methods comparison study, Atmos. Environ., 22, 1657–1663, doi:10.1016/0004-6981(88)90393-9, 1988.

Platt, U., Perner, D., Schröder, J., Kessler, C. and Toennissen, A.: The diurnal variation of NO_3, J. Geophys. Res., 86, 11965–11970, 1981.

Pleim, J. E., Bash, J. O., Walker, J. T., and Cooter, E. J.: Development and evaluation of an ammonia bidirectional flux parameterization for air quality models, J. Geophys. Res.-Atmos., 118, 3794–3806, doi:10.1002/jgrd.50262, 2013.

Plessow, K., Spindler, G., Zimmermann, F., and Matschullat, J.: Seasonal variations and interactions of N-containing gases and particles over a coniferous forest, Saxony, Germany, Atmos. Environ., 39, 6995–7007, doi:10.1016/j.atmosenv.2005.07.046, 2005.

Pope, C. A., Ezzati, M., and Dockery, D. W.: Fine-particulate air pollution and life expectancy in the United States, New Engl. J. Med., 360, 376–386, doi:10.1056/NEJMsa0805646, 2009.

Pouliot, G., Pierce, T., Denier van der Gon, H., Schaap, M., Moran, M., and Nopmongcol, U.: Comparing emission inventories and model-ready emission datasets between Europe and North America for the AQMEII project, Atmos. Environ., 53, 4–14, doi:10.1016/j.atmosenv.2011.12.041, 2012.

Putaud, J.-P., Van Dingenen, R., Alastuey, A., Bauer, H., Birmili, W., Cyrys, J., Flentje, H., Fuzzi, S., Gehrig, R., Hansson, H. C., Harrison, R. M., Herrmann, H., Hitzenberger, R., Hüglin, C., Jones, A. M., Kasper-Giebl, A., Kiss, G., Kousa, A., Kuhlbusch, T. A. J., Löschau, G., Maenhaut, W., Molnar, A., Moreno, T., Pekkanen, J., Perrino, C., Pitz, M., Puxbaum, H., Querol, X., Rodriguez, S., Salma, I., Schwarz, J., Smolik, J., Schneider, J., Spindler, G., ten Brink, H., Tursic, J., Viana, M., Wiedensohler, A., and Raes, F.: A European aerosol phenomenology – 3: Physical and chemical characteristics of particulate matter from 60 rural, urban, and kerbside sites across Europe, Atmos. Environ., 44, 1308–1320, doi:10.1016/j.atmosenv.2009.12.011, 2010.

ACPD
15, 23731–23794, 2015

Reche, C., Viana, M., Pandolfi, M., Alastuey, A., Moreno, T., Amato, F., Ripoll, A., and Querol, X.: Urban NH_3 levels and sources in a Mediterranean environment, Atmos. Environ., 57, 153–164, doi:10.1016/j.atmosenv.2012.04.021, 2012.

Sartelet, K., Debry, E., Fahey, K., Roustan, Y., Tombette, M., and Sportisse, B.: Simulation of aerosols and gas-phase species over Europe with the Polyphemus system: Part I – Model-to-data comparison for 2001, Atmos. Environ., 41, 6116–6131, doi:10.1016/j.atmosenv.2007.04.024, 2007.

Saylor, R. D., Edgerton, E. S., Hartsell, B. E., Baumann, K., and Hansen, D. A.: Continuous gaseous and total ammonia measurements from the southeastern aerosol research and characterization (SEARCH) study, Atmos. Environ., 44, 4994–5004, doi:10.1016/j.atmosenv.2010.07.055, 2010.

Schaap, M., Timmermans, R. M. A., Roemer, M., Boersen, G. A. C., Builtjes, P. J. H., Sauter, F. J., Velders, G. J. M., and Beck, J. P.: The LOTOS EUROS model: description, validation and latest developments, Int. J. Environ. Pollut., 32, 270, doi:10.1504/IJEP.2008.017106, 2008.

Schmidt, H. and Derognat, C.: A comparison of simulated and observed ozone mixing ratios for the summer of 1998 in Western Europe, Atmos. Environ., 35, 6277–6297, doi:10.1016/S1352-2310(01)00451-4, 2001.

Sciare, J., d'Argouges, O., Zhang, Q. J., Sarda-Estève, R., Gaimoz, C., Gros, V., Beekmann, M., and Sanchez, O.: Comparison between simulated and observed chemical composition of fine aerosols in Paris (France) during springtime: contribution of regional versus continental emissions, Atmos. Chem. Phys., 10, 11987–12004, doi:10.5194/acp-10-11987-2010, 2010.

Sciare, J., d'Argouges, O., Sarda-Estève, R., Gaimoz, C., Dolgorouky, C., Bonnaire, N., Favez, O., Bonsang, B., and Gros, V.: Large contribution of water-insoluble secondary organic aerosols in the region of Paris (France) during wintertime, J. Geophys. Res., 116, D22203, doi:10.1029/2011JD015756, 2011.

Seinfeld, J. H. and Pandis, S. N.: Atmospheric Chemistry and Physics: from Air Pollution to Climate Change, John Wiley, New York, 2006.

Skjøth, C. A., Geels, C., Berge, H., Gyldenkærne, S., Fagerli, H., Ellermann, T., Frohn, L. M., Christensen, J., Hansen, K. M., Hansen, K., and Hertel, O.: Spatial and temporal variations in ammonia emissions – a freely accessible model code for Europe, Atmos. Chem. Phys., 11, 5221–5236, doi:10.5194/acp-11-5221-2011, 2011.

ACPD
15, 23731–23794, 2015

Solomon, P. A., Salmon, L. G., Fall, T., and Cass, G. R.: Spatial and temporal distribution of atmospheric nitric acid and particulate nitrate concentrations in the Los Angeles area, Environ. Sci. Technol., 26, 1594–1601, doi:10.1021/es00032a016, 1992.

Stern, R.: Entwicklung und Anwendung des chemischen Transportmodells REM/CALGRI D. Breichte zum UBA Forschungsvorhaben 298 41 252, Freie Universität Berlin, Institut für Meteorologie, 2003.

Stohl, A., Haimberger, L., Scheele, M. P., and Wernli, H.: An intercomparison of results from three trajectory models, Meteorol. Appl., 8, 127–135, doi:10.1017/S1350482701002018, 2001.

Sutton, M., Dragosits, U., Tang, Y., and Fowler, D.: Ammonia emissions from non-agricultural sources in the UK, Atmos. Environ., 34, 855–869, doi:10.1016/S1352-2310(99)00362-3, 2000.

Takahama, S., Wittig, A. E., Vayenas, D. V., Davidson, C. I., and Pandis, S. N.: Modeling the diurnal variation of nitrate during the Pittsburgh Air Quality Study, J. Geophys. Res., 109, D16S06, doi:10.1029/2003JD004149, 2004.

Trebs, I., Meixner, F. X., Slanina, J., Otjes, R., Jongejan, P., and Andreae, M. O.: Real-time measurements of ammonia, acidic trace gases and water-soluble inorganic aerosol species at a rural site in the Amazon Basin, Atmos. Chem. Phys., 4, 967–987, doi:10.5194/acp-4-967-2004, 2004.

Trebs, I., Andreae, M. O., Elbert, W., Mayol-Bracero, O. L., Soto-García, L. L., Rudich, Y., Falkovich, A. H., Maenhaut, W., Artaxo, P., Otjes, R., and Slanina, J.: Aerosol inorganic composition at a tropical site: discrepancies between filter-based sampling and a semi-continuous method, Aerosol Sci. Tech., 42, 255–269, doi:10.1080/02786820801992899, 2008.

Van Der Gon, H. D., Visschedijk, A., and Appelhans, F. J.: A high resolution European emission data base for the year 2005, available at: http://www.csb.gov.tr/db/necen/editordosya/file/NEC/MACC_Training/TNO_PAREST.pdf (last access: 12 June 2015), 2010.

Vayenas, D. V., Takahama, S., Davidson, C. I., and Pandis, S. N.: Simulation of the thermodynamics and removal processes in the sulfate-ammonia-nitric acid system during winter: implications for $PM_{2.5}$ control strategies, J. Geophys. Res., 110, D07S14, doi:10.1029/2004JD005038, 2005.

Vrekoussis, M., Kanakidou, M., Mihalopoulos, N., Crutzen, P. J., Lelieveld, J., Perner, D., Berresheim, H., and Baboukas, E.: Role of the NO_3 radicals in oxidation processes in the

ACPD
15, 23731–23794, 2015

eastern Mediterranean troposphere during the MINOS campaign, Atmos. Chem. Phys., 4, 169–182, doi:10.5194/acp-4-169-2004, 2004.

Wesely, M. L.: Parameterization of surface resistances to gaseous dry deposition in regional-scale numerical models, Atmos. Environ., 23, 1293–1304, doi:10.1016/0004-6981(89)90153-4, 1989.

Wichink Kruit, R. J. (Roy), van Pul, W. A. J., Otjes, R. P., Hofschreuder, P., Jacobs, A. F. G., and Holtslag, A. A. M.: Ammonia fluxes and derived canopy compensation points over non-fertilized agricultural grassland in the Netherlands using the new gradient ammonia – high accuracy – monitor (GRAHAM), Atmos. Environ., 41, 1275–1287, doi:10.1016/j.atmosenv.2006.09.039, 2007.

Yao, X., Hu, Q., Zhang, L., Evans, G. J., Godri, K. J., and Ng, A. C.: Is vehicular emission a significant contributor to ammonia in the urban atmosphere?, Atmos. Environ., 80, 499–506, doi:10.1016/j.atmosenv.2013.08.028, 2013.

Yin, J. and Harrison, R. M.: Pragmatic mass closure study for $PM_{1.0}$, $PM_{2.5}$ and PM_{10} at roadside, urban background and rural sites, Atmos. Environ., 42, 980–988, doi:10.1016/j.atmosenv.2007.10.005, 2008.

Zhang, L., Wright, L. P., and Asman, W. A. H.: Bi-directional air–surface exchange of atmospheric ammonia: a review of measurements and a development of a big-leaf model for applications in regional-scale air-quality models, J. Geophys. Res., 115, D20310, doi:10.1029/2009JD013589, 2010.

ACPD
15, 23731–23794, 2015

Table 1. Periods with available measurements for the gaseous and particulate inorganic compounds from 1 April to 31 December 2010.

Species	Period (sampling time)
NH_3	20 May–31 Dec 2010 (< 1 h)
HNO_3	1 Apr–31 Dec 2010 (< 1 h)
NH_4^+ NO_3^- SO_4^{2-}	1 Apr–10 Sep 2010 (24 h)

ACPD
15, 23731–23794, 2015

Table 2. Statistical results at our urban background sites over the whole period (all statistical metrics are defined at the beginning of Sect. 4; MO is the observed concentration mean, *N* the data coverage).

Species	Case	MO	MB	NMB (%)	RMSE	NRMSE (%)	*R*	*N* (%)
NH_3* (ppb)	MOD	4.0	−3.0	−75	3.9	99	0.42	64
	MOD-noIDF		−3.1	−79	4.1	103	0.39	64
	MOD-nodep		−1.8	−46	3.2	82	0.45	64
HNO_3* (ppb)	MOD	0.3	+0.5	+195	0.8	320	0.56	81
	MOD-noIDF		+0.3	+120	0.6	219	0.36	81
SO_2* (ppb)	MOD	0.5	+1.0	+194	1.6	303	0.38	83
	MOD-noIDF		−0.1	−20	0.9	170	0.25	83
Ammonium ($\mu g\,m^{-3}$)	MOD	1.2	+0.4	+35	0.9	70	0.84	54
	MOD-noIDF		+0.3	+23	0.8	64	0.84	54
Nitrate ($\mu g\,m^{-3}$)	MOD	2.1	+0.4	+19	2.2	109	0.81	54
	MOD-noIDF		+0.0	+1	2.1	101	0.81	54
Sulfate ($\mu g\,m^{-3}$)	MOD	2.0	+1.0	+48	1.5	74	0.59	54
	MOD-noIDF		+0.9	+42	1.4	69	0.61	54
F-NHx (ppb)	MOD	5.5	−4.1	−75	4.7	87	0.51	37
	MOD-noIDF		−4.4	−80	5.0	92	0.48	37
S_{ratio}	MOD	0.3	+0.2	+60	0.3	73	0.46	48
	MOD-noIDF		−0.1	−29	0.2	55	0.33	48
GR ($ppb\,ppb^{-1}$)	MOD	12.6	−11.4	−90	14.2	112	0.37	36
	MOD-noIDF		−11.2	−88	14.0	111	0.33	36
TNH_3 (ppb)	MOD	6.4	−3.6	−56	4.4	70	0.43	37
	MOD-noIDF		−3.9	−61	4.7	74	0.40	37
TNO_3 (ppb)	MOD	1.1	+0.8	+71	1.3	123	0.78	47
	MOD-noIDF		+0.3	+31	1.1	97	0.79	47

* Statistics based on hourly data (otherwise, daily data are used).

ACPD
15, 23731–23794, 2015

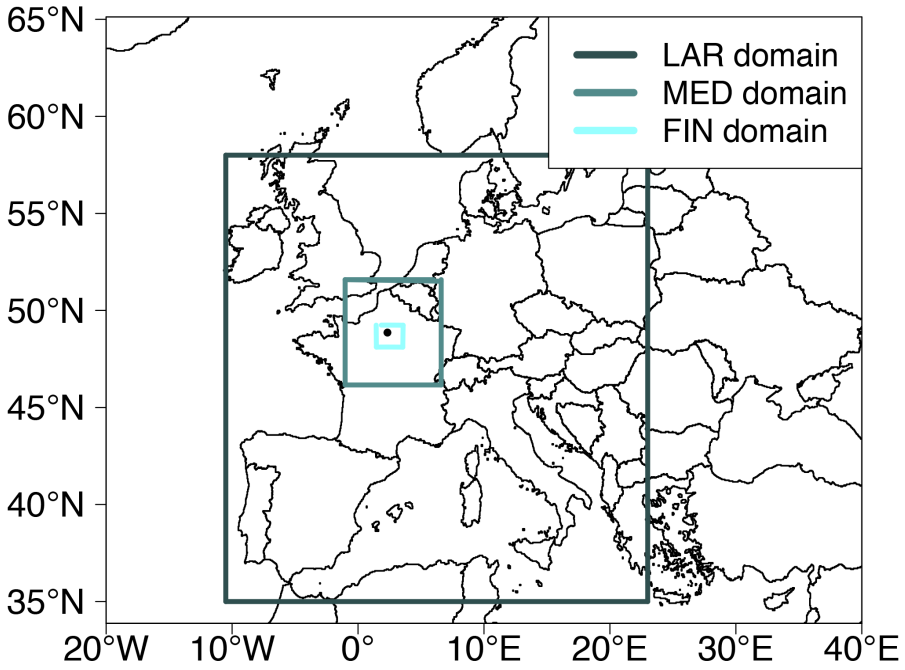

Figure 1. Nested domains (the black points in the finest domain indicates Paris).

ACPD
15, 23731–23794, 2015

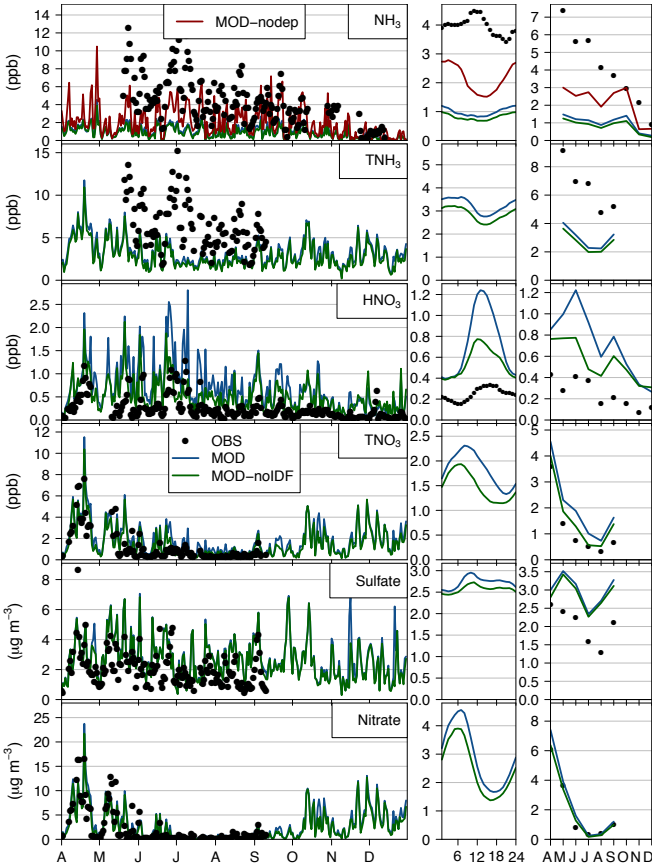

Figure 2. Observed and modelled daily concentrations (left panel), diurnal profiles (middle panel), and monthly concentrations (right panel). MOD-nodep results are only shown for NH_3. Note: CHIMERE monthly concentrations are computed including only days with available observational data.

ACPD
15, 23731–23794, 2015

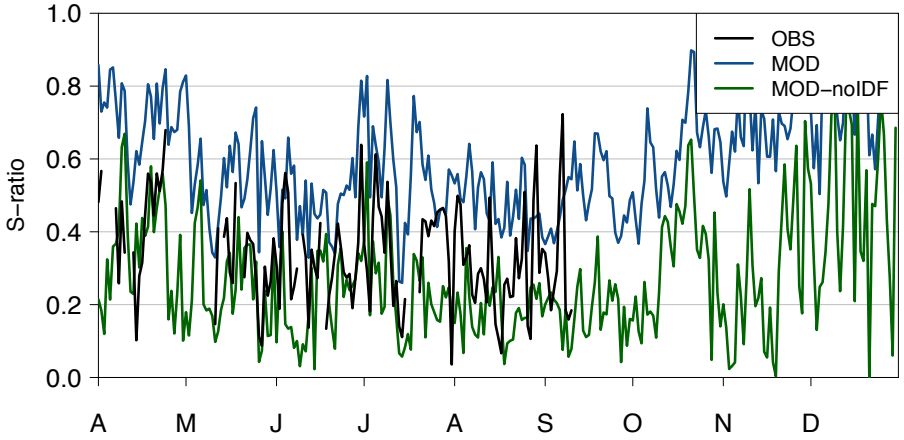

Figure 3. Observed and modelled (with – MOD case – and without – MOD-noIDF case – emissions over the Paris region) daily *S* ratio in Paris.

ACPD
15, 23731–23794, 2015

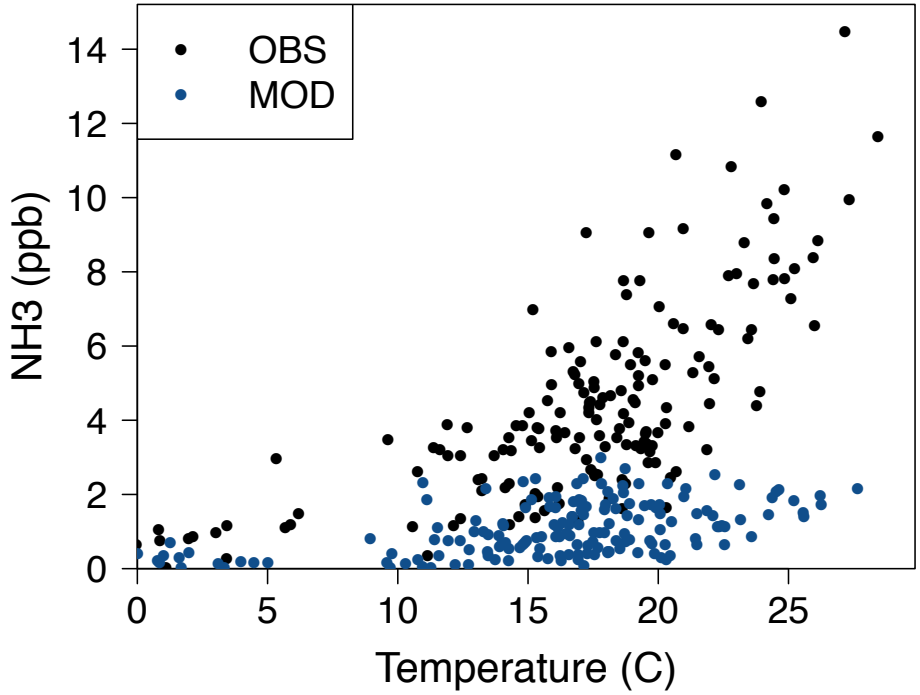

Figure 4. Daily observed (respectively modelled) NH_3 concentrations against observed (respectively modelled) temperature in Paris (for the model, only days with available observations are plotted).

ACPD
15, 23731–23794, 2015

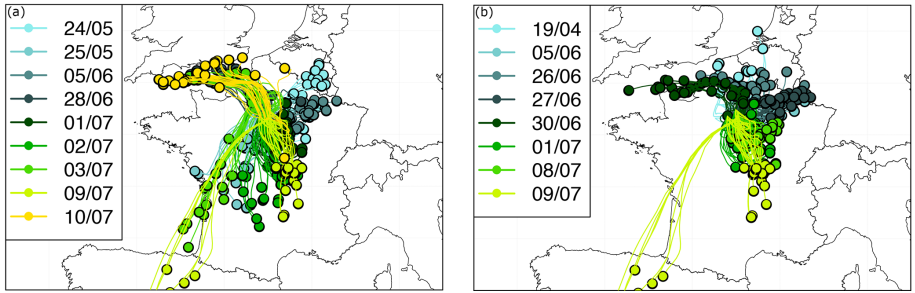

Figure 5. Back-trajectories at D-1 (one day before reaching Paris) associated with highest **(a)** NH_3 (left panel) and **(b)** HNO_3 (right panel) episodes (highest episodes being selected according to daily concentrations above the 97th percentile of all daily measurements, i.e. 9.2 and 0.9 ppb for NH_3 and HNO_3, respectively). For clarity, only back-trajectories of 7 particles around the center of Paris are plotted, each 6 h (i.e. 28 back-trajectories per day).

ACPD
15, 23731–23794, 2015

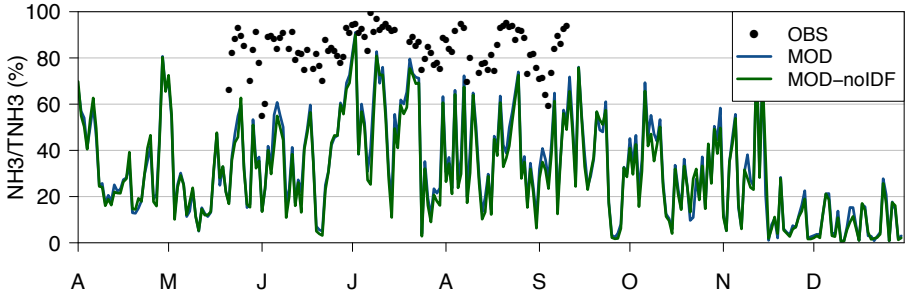

Figure 6. Daily NH_3/TNH_3 ratios in observations (points) and simulations (colored lines).

ACPD
15, 23731–23794, 2015

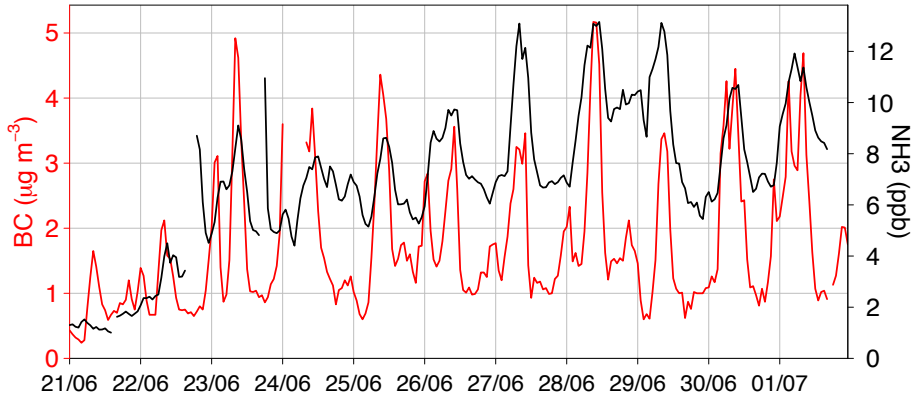

Figure 7. Observed BC (in red) and NH_3 (in black) hourly concentrations at LHVP during the end of June.

ACPD
15, 23731–23794, 2015

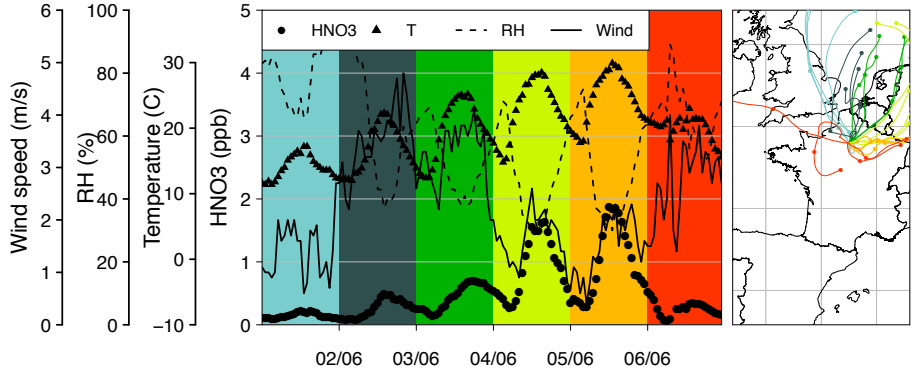

Figure 8. Hourly concentrations of HNO_3 at LHVP and wind speed, RH and temperature during early June 2010 (left panel), and associated 48 h back-trajectories (one point every 24 h) coloured by the day of arrival (i.e. red is for 06/06).

ACPD
15, 23731–23794, 2015

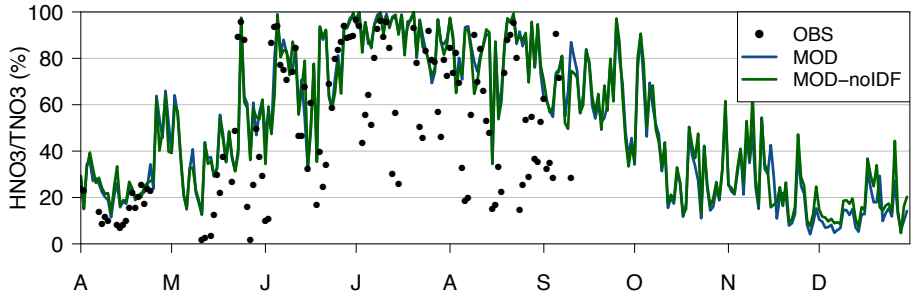

Figure 9. Daily HNO_3/TNO_3 ratios.

ACPD
15, 23731–23794, 2015

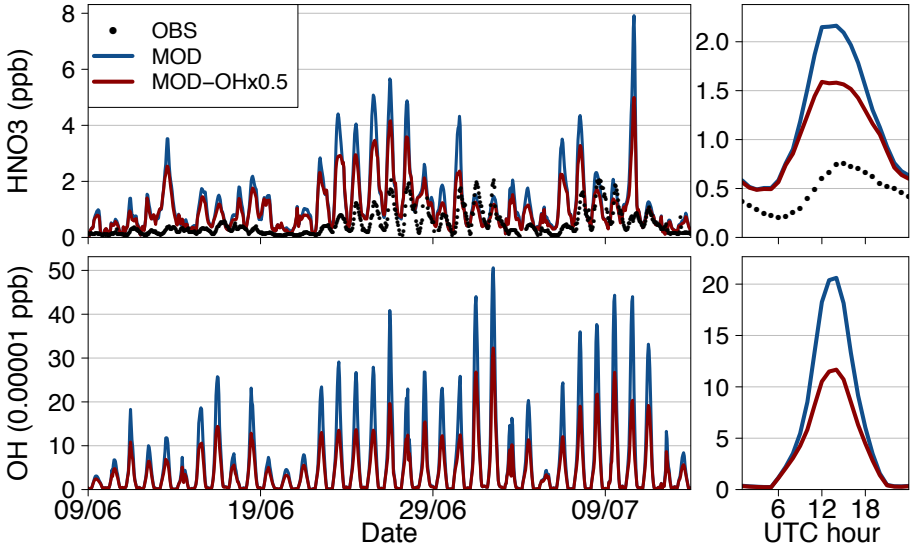

Figure 10. HNO_3 and OH hourly concentrations (left panel) and diurnal profiles (right panel) at the LHVP site.

ACPD
15, 23731–23794, 2015

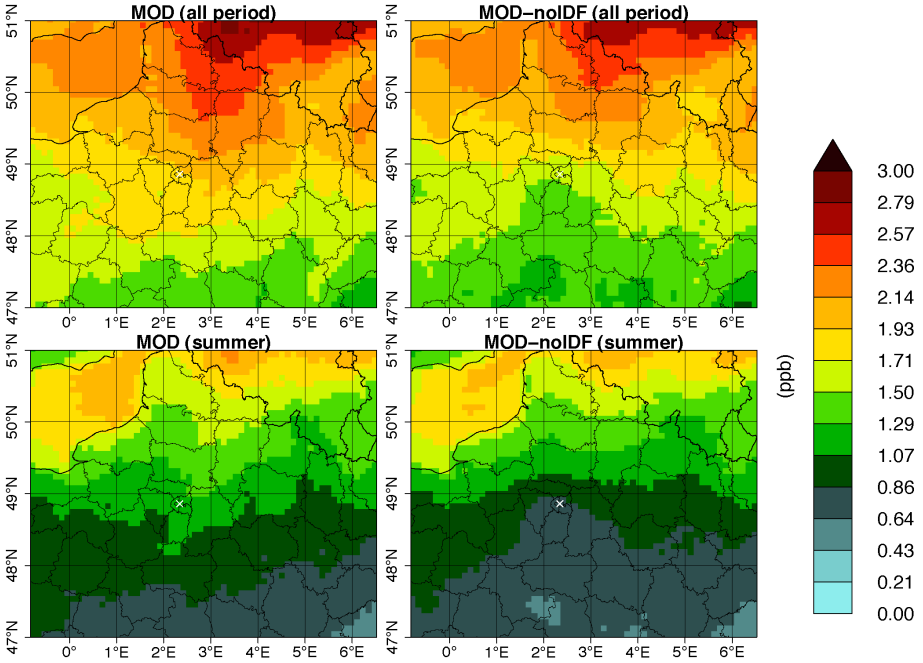

Figure 11. TNO_3 mean concentration over the MED domain, for both MOD and MOD-noIDF cases, during the whole period (top) and only summer (bottom). The white cross indicates the Paris center.

ACPD
15, 23731–23794, 2015

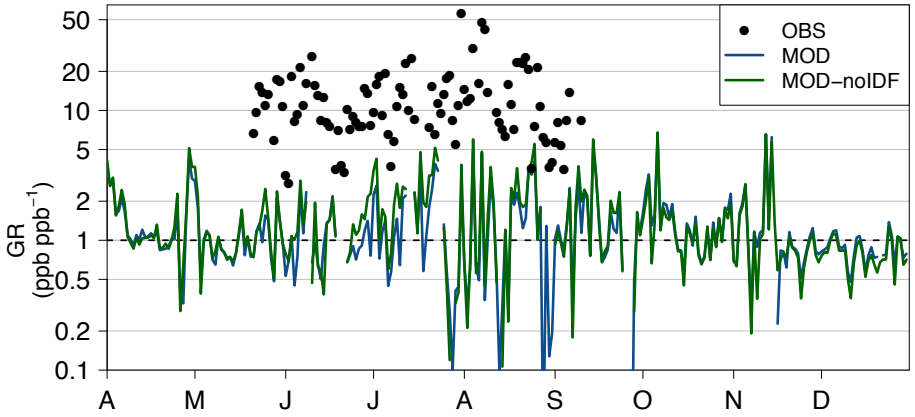

Figure 12. Observed and modelled daily GR.

ACPD
15, 23731–23794, 2015

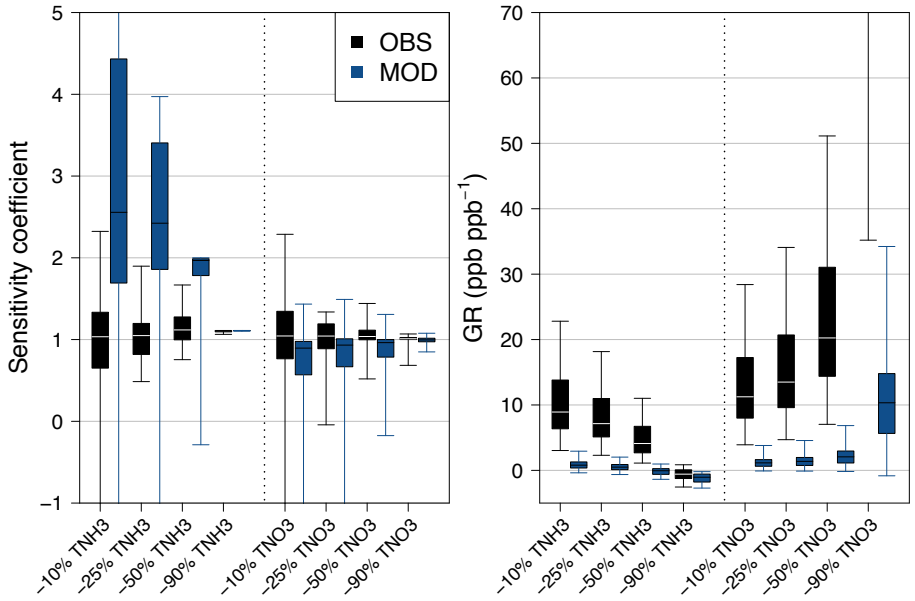

Figure 13. Sensitivity coefficient S_x of nitrate formation due to different changes (−10, −25, −50 and −90 %) in TNH_3 and TNO_3 concentrations (left panel) and resulting GR (right panel) during the period from 15 May to 10 September 2010. Experimental data (OBS) in black, modelled data (MOD) in blue. Box plots indicate 5th, 25th, 50th, 75th and 95th percentiles.

ACPD
15, 23731–23794, 2015